EUROVOLC

European Network of

Observatories and Research Infrastructure for Volcanology

Deliverable Report

D5.2: Best practices ground-based measurements in volcanic plumes
Best practices for techniques to measure fluxes and compositions in volcanic plumes

Work Package:	Consolidation of geochemical gas monitoring across VOs	
Work Package number:	5	
Work Package leader:	Fausto Grassa	
Task (Activity) name:	Best practices for techniques to measure fluxes and compositions in volcanic plumes.	
Task number:	5.2	
Responsible Activity leader:	UMAN (M. Burton)	
Lead beneficiary:	INGV	
Author(s)	B. McCormick Kilbride, S. Moune, G. Salerno, B. Esse, A. Burtin, M. Liuzzo, F. Viveiros, A. Di Muro, M.A. Pfeffer, C. Silva, M. Burton	
Type of Deliverable:	Report [X] Prototype [ ]	Demonstrator [ ] Other [ ]
Dissemination level:	Public [X] Prog. Participants [ ]	Restricted Designated Group [ ] Confidential (consortium) [ ]

Contents

1. Summary

This report summarises the activities undertaken in the framework of Task 5.2 (WP5) of the EUROVOLC project. Our aim has been to contribute to the development of community of best practices for the monitoring of volcanic gases in the field, with a focus on remote sensing of sulfur dioxide (SO_2) emissions and in situ monitoring of gas chemical composition. The two principal techniques with which our work has been concerned are ultraviolet (UV) absorption spectroscopy and the deployment of multi-component gas analyser systems (MultiGAS). Our recommendations encompass instrument design and construction, field deployments and measurement protocols, and data post-processing and interpretation. The work described herein is complementary to Task 5.1 (Best practices for direct sampling techniques and analysis of fumarolic gases) and Task 5.3 (Integration of geochemical dataset of atmospheric gases), also in WP5.

The original goal of Task 5.2 was to undertake a multi-institution field campaign on an active volcano, where workers from several teams could make several days of measurements in parallel, developing in-person discussions around best practices related to instrument calibration and setup (before going into the field), field deployments and data acquisition, and subsequent data treatment. This campaign was scheduled for May 2020 and would have taken place on Vulcano Island, Italy, an accessible active volcano for all partner institutions. However, the spread of COVID-19 and the announcement of a global pandemic imposed substantial limitations on our plans. The proposed field campaign was postponed, on the basis of hoped-for extensions to the project. Despite continuing exploration of scheduling and travel over the intervening months, in March 2021 at a task meeting during the EUROVOLC third annual meeting, the Task 5.2 team concluded that no multi-institution international travel would be feasible on the timescale of the EUROVOLC project. This has proven to be the case, with varying rates of vaccination and case numbers, plus ever-shifting travel restrictions and quarantine requirements between different nations hampering our efforts. Since spring 2021, therefore, we have opted to focus instead on developing ideas of best practices based on sharing and intercomparing existing datasets. While this is perhaps a less complete exploration of best practices than we had hoped, we believe that the following report makes a series of tractable recommendations that can be adopted by future workers, debated across our community, and explored by various groups once the global pandemic has eased.

This report is composed of the following sections:

- **State of the art.** We outline the motivation of monitoring volcanic gas emissions, focusing on SO_2 emission rate and plume chemistry as key variables of interest.
- **Results.** We share the results of our inter-comparison exercises, which we devised to explore how different groups process UV spectroscopy and MultiGAS data to obtain, respectively, SO_2 emission rates and gas plume compositions (molar ratios). These exercises are based on data acquired in past field campaigns undertaken by individual partner organisations.
- **Discussion.** We explore some of the issues raised by our intercomparison exercises, including light dilution and its impact on UV spectroscopy, and the influence on time window length, choice of regression method, and background characterisation in estimating plume composition from MultiGAS measurements.
- **Recommendations of best practice.** Finally, we conclude with a series of tractable recommendations that should be either adopted or more fully explored by the global

volcanological community, both in research and operational monitoring, to improve the accuracy and reliability of plume measurements in years to come.

The participating groups (and abbreviations uses throughout the report) are as follows:

- Istituto Nazionale di Geofisica e Vulcanologia, Sezione di Palermo (INGV-PA)
- Istituto Nazionale di Geofisica e Vulcanologia, Osservatorio Etneo (INGV-OE)
- Centro de Informação e Vigilância Sismovulcânica dos Açores (CIVISA)
- Institut de Physique du Globe de Paris / Observatoire Volcanologique et Sismologique de Guadeloupe (IPGP-OVSG)
- Institut de Physique du Globe de Paris / Observatoire Volcanologique et Sismologique de Piton de la Fournaise (IPGP-OVPF)
- Icelandic Meteorological Office (IMO)
- University of Manchester (UMAN)

2. State of the art

Monitoring volcanic gas emissions is a key means of evaluating the level of unrest at volcanoes (Chiodini et al., 1995; Edmonds et al., 2003a, 2003b; Oppenheimer et al., 2011; Sparks et al., 2012). Magmas rising through the crust undergo decompression and therefore volatile exsolution ("first boiling"), leading to changes in the chemical composition and emission rate (flux) of gases at the surface. Changes in gas emissions can also arise because of magma reservoir processes, such as recharge by "fresh" undergassed magma, magma mixing, or extended periods of crystallization ("second boiling"). Volcanic gases are the only direct chemical probes of magmas at depth before eruptions start (Edmonds, 2021). Over long-duration intervals (>years) it is anticipated that individual volcanoes may be characterised by stable CO_2/SO_2 set by deep processes, e.g., storage depth of actively degassing magma or magma volatile budgets inherited from source regions (de Moor et al., 2017; Aiuppa et al., 2019). However, fluctuations in CO_2/SO_2 away from this 'background' can then be usefully interpreted for hazard assessment, for example, increases in CO_2/SO_2 often accompany mafic recharge and the CO_2-dominated degassing of parental magmas, while subsequent decreases in CO_2/SO_2 accompany magma ascent towards the surface as CO_2 is exhausted in the magma and SO_2 exsolution begins. The time-dependence of such changes can aid interpretation of the responsible processes.

A large body of work has grown around the idea that changes in gas emissions can be interpreted in terms of subsurface processes, whether in the reservoir or volcanic conduit, and accordingly much focus has been placed on using these changes in emissions to warn of, or even forecast, future volcanic eruptions. Characteristic precursory 'spikes' in CO_2/SO_2 have been observed to precede eruptions at several volcanoes worldwide (Aiuppa et al., 2007, 2009; de Moor et al., 2016; Werner et al., 2019). The accurate quantification of spatial and temporal variations in volcanic outgassing is also important to evaluate the contribution of volcanoes to climatic or environmental change (Oppenheimer et al., 2011; Mason et al., 2017; Werner et al., 2019).

Many techniques are available to monitor changes in volcanic gas emissions, including direct sampling of gases for diverse laboratory analyses (Giggenbach & Goguel, 1988; Giggenbach & Poreda, 1993; Fischer et al., 1998; Vaselli et al., 2010), in situ (real-time) measurements of plume composition (Aiuppa et al., 2007, 2009; de Moor et al., 2016; Liu et al., 2020), and remote sensing methods (Edmonds et al., 2003a,b; Galle et al., 2003; Salerno et al., 2009). The application of these techniques varies globally, according to

the volcanic or environmental conditions and the available funding or resources. Many research teams and volcano observatories have developed their own protocols concerning field deployment of instruments, data acquisition, (post-) processing, data reporting and archival.

Globally, the volume of data generated in the monitoring of gas emissions in growing, as more institutions adopt continuous monitoring, or the deployment of multiple instrument types, or a shift towards automated monitoring across multiple volcanoes in a region of interest (Edmonds et al., 2003b; Arellano et al., 2008; Salerno et al., 2009; Galle et al., 2010; Werner et al., 2019; Fischer & Aiuppa, 2020; Arellano et al., 2021). Alongside this explosion of new data, there must be a corresponding increase in the attention to how data is collected, processed, and stored. It is important for the global volcanological community, whether in research or in operational monitoring, to compare the different approaches undertaken and ensure consistency, thus ensuring that the data being collected is of the highest quality and can be a firm basis for interpreting the state of volcanic unrest or the evolution of magmatic processes. For this reason, the third element of Work Package 5 aims to tackle this challenge: "Task 5.3 Integration of geochemical datasets of atmospheric gases", harmonizing growing volcanic gas data sets and building new repositories that can sit within the EPOS framework. Its final target is to propose a structure of database for geochemical data, obtained from field surveys and/or with subsequent laboratory analyses.

2a. Sulfur dioxide flux by UV spectroscopy

Sulfur dioxide (SO_2) is the third most abundant volatile species in magmas after water (H_2O) and carbon dioxide (CO_2). It is the most frequently monitored gas species. However, owing to distinctive absorption structures at ultraviolet wavelengths and because SO_2 is present in the free troposphere only at very low concentrations with respect to the abundances found in the plumes of actively degassing volcanoes (0.0001 - 0.024 ppm and 0.1-0.3 ppm, respectively). Since the 1970s these two factors have led to widespread remote observations of SO_2 gas emissions from volcanic vents. SO_2 starts exsolving from magmas at shallow crustal depths (~140 MPa, Oppenheimer et al., 2011), making changes in SO_2 emission rate at the surface a sensitive tracer of magma ascent, conduit permeability, and other important parameters (Salerno et al., 2009; Edmonds et al., 2003a, 2003b). This is particularly important at 'open vent' volcanoes where gases escaping from the magma reach the surface without extensive modification, in contrast with quiescent volcanoes where rising gases may interact with a well-developed hydrothermal envelope (Symonds et al., 1994; Oppenheimer et al., 2011; Edmonds, 2021).

Since 2003 a series of instruments have been developed to facilitate monitoring of SO_2 fluxes at high temporal resolution and varying degrees of automation (Stoiber et al., 1983; Edmonds et al., 2003a,b; Galle et al., 2003; Mori & Burton, 2006; Salerno et al., 2009; Galle et al., 2010; Arellano et al., 2021). In this report, we will focus on the classical COSPEC approach of traverse SO_2 flux measurement, rather than scanning or the UV camera, though we will note where our findings and conclusions can be more generally applied. An effective way to monitor SO_2 fluxes are automated scanning UV spectrometers, ideally a network of multiple instruments allowing good plume coverage and triangulation of plume position (lat/lon/altitude). Various sources of wind data can be chosen, depending on local conditions, such as direct anemometer or sonde measurements, or simulated wind fields.

UV cameras can provide an independent estimate of SO_2 emissions, albeit often with larger uncertainties. An advantage of the camera over scanning systems is the better temporal resolution, which is helpful for studies of conduit dynamics, short-lived (<minute) changes in gas flux, or integrated with geophysical data streams such as seismicity or infrasound (Tamburello et al., 2011, Nadeau et al., 2011; McGonigle et al.,

2017). Cameras can also quantify plume velocity (e.g., via particle motion tracking, e.g., Peters et al., 2015). Ideally, UV cameras are deployed sufficiently close enough to the volcanic vent (< 3km, but variable depending on local conditions) to minimise light dilution, yet also far enough away to fit the entire plume into the field of view (Varnam et al., 2020). If a UV camera is co-located with a spectrometer, the camera images may be calibrate using spectrometer measurements rather than the more widely adopted gas calibration cells.

Ultraviolet absorption spectroscopy is based on the observation that molecules being irradiated by electromagnetic radiation can change their energy by performing quantum transitions to electronic, vibrational, and rotational excited states (Platt & Stutz, 2008). As the energy levels of these states depend on the molecule type, every molecule will absorb light at distinct wavelengths. The quantitative description of the absorption spectroscopy is given by the Lambert-Beer law, which describes the exponential decrease in the intensity of the electromagnetic radiation when propagating through matter. SO_2 has a strong absorption of light in the ultraviolet region making open-path passive measurements of volcanic SO_2 easily achievable. Inverting open-path UV spectra applying the differential optical absorption spectroscopy (DOAS) or intensity fit techniques, raw spectra are converted in SO_2 Column Amount (CA; molecules/cm2 or ppm m). A profile of SO_2 CA measured orthogonal to the plume can be integrated to achieve a cross-sectional concentration and this can be multiplied by plume speed (in practice, wind speed) to estimate the SO_2 emission rate from the volcanic vent.

The uncertainty in the retrieved CA is determined by several factors and may arise due to: (i) the instrumental configuration and noise; (ii) environmental factors affecting the detector (e.g., temperature); (iii) the size, structures and temperature of the differential literature absorption cross-sections; (iv) the number of absorbers in the investigated spectral region; (v) the light path between the sun and the detector (light dilution); (vi) the intensity of the light signal transmitted through the atmosphere; and the (vii) retrieval wavelength region (Kern et al., 2010, 2012). Uncertainty in SO_2 mass flux mainly depends in the error of wind-speed (Edmonds et al., 2008).

Under certain conditions the efficacy of UV measurements is reduced, for example, low sunlight due to high latitude, season, time of day, or extensive cloud cover obscuring the volcanic plume. Strongly condensing, particle-rich or otherwise opaque plume dramatically reduce UV transmission. In some cases, solutions can be developed but often these departures from ideal measurement conditions and may result in gaps in data time series. Typical remote sensing measurements of SO_2 in a plume assume a straight ray-path from the light source (background sky-light) through the plume and to the instrument. However, in reality this is often not the case. If the plume is optically thick (e.g., due to condensation or from the presence of volcanic ash) then multiple scattering within the plume can increase the length of the light path through the plume, enhancing the SO_2 signal so that the slant column density (SCD) is overestimated. This is difficult to correct for, but some attempts using radiative transfer models have been made (Kern et al. 2013). Conversely, scattering of light between the plume and the instrument can decrease the measured SCD. Along the observation path between the instrument and the plume, "plume" light is scattered out of the field of view of the instrument while "non-plume" light is scattered in. This dilutes the plume signal and is commonly referred to as light dilution. The magnitude of this effect increases with the optical depth of the atmosphere and the distance from the plume. Additionally, as the strength of Rayleigh scattering depends on the wavelength of the light as λ^{-4}, light dilution is much stronger at shorter wavelengths. The effects of light dilution can be mitigated by ensuring the distance to the plume is as short as possible and by analysing the spectra at longer wavelengths, however it is best to correct the

measurement either through full radiative transfer (Kern et al., 2012) or through corrections with dual wave-band analysis (Mori et al., 2006; Varnam et al., 2020).

In addition to radiative transfer issues, uncertainties in the plume speed and geometry can also influence SO_2 flux measurements. The calculated flux is directly proportional to the plume (Wind) speed used, making this a key parameter that is difficult to measure directly. Many scanning systems rely on global or regional weather models to provide wind speeds (Salerno et al., 2009; Galle et al., 2010), however these are notoriously inaccurate near to topography (such as a volcanic edifice). Similarly, the use of ground-based weather stations can lead to systematic errors as the wind speed measured near to the ground can differ dramatically from the wind at the plume altitude. The best method is to measure the speed directly, either through analysis of video imagery or by correlating fluctuations in the plume concentration measured at two points separated downwind of the plume (McGonigle et al., 2005). Knowledge of the plume geometry is another source of uncertainty for scanning measurements. To convert a scan to a flux requires assumptions on the plume geometry. Typically, it is assumed that either the plume is at a fixed distance from the scanner (regardless of the location in the scan arc) or that it is at a fixed altitude. Neither of these assumptions truly represent the physical shape of a plume but must be assumed in place of additional information. The plume can be located in space geometrically if it is seen by more than one scanner (Galle et al., 2010; Platt et al., 2018). Finally, though it is not common, the distribution of SO_2 in the plume can be retrieved through tomographic techniques (Kazahaya et al., 2008, Wright et al., 2008), removing these geometrical sources of uncertainty.

2b. In-situ plume composition by MultiGAS

Since a volcanic plume is necessarily a mixture of volcanic gases and air, the remote sensing of H_2O and CO_2 is limited by their high atmospheric concentration, particularly at light-path lengths longer than a few hundred metres. Open-path Fourier transform infrared (OP-FTIR) spectroscopy has been used to measure H_2O-CO_2-SO_2 in volcanic plumes via remote sensing, but this method is best suited to scenarios where active lava can act as a thermal infrared source such as lava flows, lakes, or high temperature domes (Burton et al., 2000; Allard et al., 2005; Edmonds, 2008). At volcanoes where no lava is exposed at the surface, or the vent cannot be so closely approached, changes in the emission of H_2O and CO_2 must therefore be targeted with in situ methods, measuring plumes close to the point of emission to minimize mixing with the atmosphere, chemical reactions, or condensation. Multi-component Gas Analyser Systems (MultiGAS, Shinohara, 2005; Aiuppa et al., 2005) have been developed for this purpose.

The MultiGAS system is a custom-made sensor box, allowing high rate (1 Hz) real-time detection of CO_2 with NDIR spectroscopy and an array of electrochemical sensors to measure SO_2, H_2S, HCl, H_2 and CO concentrations. All sensors and electronics are located within a robust plastic Pelicase or similar. These instruments have become widely used for gas studies and monitoring on various volcanoes worldwide (Shinohara et al., 2005; Aiuppa et al., 2007, 2009; Werner et al., 2013; Shinohara, 2013; de Moor et al., 2016; Liu et al., 2020). The precision on measured concentrations is typically 5-10%. Atmospheric pressure is determined with the sensor installed on the CO_2 spectrometer. The MultiGAS also includes a GPS receiver to track the device's position at 1 Hz and a relative humidity (RH) sensor, permitting water vapor concentration to be determined following the procedure described in Moussallam et al. (2017). The H_2O sensor can be fixed internally or externally, the latter option allowing minimizing the potential influence of steam condensation in the MultiGAS inlet tubing. H_2O concentration can be also measured via NDIR

spectroscopy. The inlet tube is connected to a PTFE filter (to avoid ingestion of particle matter into the sensors) and the instrument is placed downwind of the vent, within the air-diluted plume, and between 20 cm to 1 m height above the ground to avoid the influence of soil degassing. The gas emissions are actively pumped to the spectrometer and electrochemical sensors at a constant flow rate of 1 to 1.5 l/min. Care should be taken not to place the sensor too close to the point of emissions to avoid condensation buildup or sensor saturation. The instrument should be located where persistent exposure to the plume can be achieved; this is particularly important where time is limited in the field area (e.g., for safety reasons during periods of elevated activity). Where there are multiple points of emission or highly changeable wind fields, multiple MultiGAS instruments may be placed around a crater rim to ensure continuous temporal monitoring can be achieved, though of course this must be balanced against resource constraints. The instrument can also be carried through a series of plumes on foot ("walking traverses") and modified versions are increasingly being deployed on unoccupied aerial systems (UAS, "drones," e.g., James et al., 2020; Liu et al., 2020). Long acquisition windows (i.e., continuous or repeated measurements over >weeks) offer the potential to understand long-term "baseline" plume compositions, which are important to determine in order to robustly detect anomalous excursions which may indicate possible shifts in volcanic activity.

Post-processing of MultiGAS data involves such operations as background correction, the use of linear regressions to derive molar composition ratios, and temporal shifts or filtering to improve correlation between gas species. The open-source software Ratiocalc (Tamburello, 2015) has been developed and made available for community use, though other groups use their own protocols. In post-processing, gas ratios are derived using linear regressions between two species (e.g., CO_2 and SO_2), with different regression methods adopted, not always consistently, between groups and between campaigns. The axis intercepts of linear regressions between two species of interest can be used to define their background concentration in the ambient atmosphere or, alternatively, the MultiGAS can be deployed outside the volcanic plume for a period to measure the background concentration of trace gases directly; a correction of the measured in-plume concentrations can be made as a result. The use of gas ratios is to overcome the effect of plume dilution, and since this assumes that ratios are conservative (over the time period since emission) measurements should be undertaken as close to point of emissions as possible.

Not all the sensors used in the MultiGAS have the same response time. Indeed, the t90 behavior (the time required to reach 90% of the final signal following a step change in gas abundance) varies widely between sensors (Roberts et al., 2014). Usually, the CO_2 NDIR sensor has more conservative behavior and a faster response compared to electrochemical sensors (Tamburello et al., 2019). Gas pulses with a duration shorter than the t90 time of a sensor are not well-captured. To overcome this, measured concentration datasets can be time-shifted and subjected to a low-pass filter. The Ratiocalc software facilitates straightforward application of filtering and temporal shifting, by allowing the user to view two overlain gas concentration time series and exploring the improvements in correlation coefficient that can be achieved by adjusting the shift. We must acknowledge the element of subjectivity involved in these temporal shifts: different shifts can be chosen by different users viewing the same data set (see further discussion below).

All the sensors contained in a MultiGAS unit must be calibrated regularly, before fieldwork and on return from the field. It is important to recognize that sensor response can be pressure dependent and where calibrations are made at different pressures (e.g., sea-level labs versus volcanoes at higher elevation) account of this must be taken.

3. Inter-comparison results

3a. SO2 emission rate – Etna

These data were provided by INGV-OE and have been studied by the INGV-OE and UMAN teams. The data consist of 282 zenith open-path ultraviolet spectra remotely collected passively in the bulk volcanic plume of Mt Etna during 21st July 2006. Ultraviolet measurements were obtained using an USB2000 Ocean Optics spectrometer. The instrument comprises a 2048-pixel detector array and diffraction grating with 3600 grooves per mm, which, combined with a 200 µm entrance slit, delivers a spectral resolution of ~1.3 nm (Full Width at Half Maximum, FWHM) in the 296–375 nm wavelength range. As in the more common COSPEC method (Williams-Jones et al, 2008), open-path UV spectra were collected traversing beneath the plume by helicopter. The instrument was mounted inside a helicopter and connected via fiber optic cable to a telescope (8 mrad field of view) that was taped to the outer window of the helicopter and oriented to point vertically upwards. Four airborne traverses were carried out between 08:57 and 09:14 UT, approximately 4 km downwind of the summit crater. Optimal integration time for the collection of spectra was 100 ms and 50 spectra were co-added to improve the signal to noise ratio. Spectra were time and position-stamped using a USB GPS receiver. Clear sky and dark spectra were collected outside of plume at the start of each traverse.

UV spectra were collected while Mt Etna was in a stage of eruptive activity. The July 2006 eruption lasted only 10 days, from 14 to 24 July, with lava flows and vigorous explosive activity occurring along a short eruptive fissure that opened on the lower ESE flank of the South East Crater (SEC) cone (Bonforte et al., 2008). The explosive activity was fed by a cluster of vents located at ~3150 m a.s.l., whereas lava output occurred on the same flank but at lower elevation (~3020 m; Neri et al., 2006; Behncke et al., 2008). This eruptive phase culminated with a short episode of lava fountaining on 20 July. As with the 2004-05 eruption, the onset of this eruptive phase was not coupled with any significant geophysical change (i.e., seismicity and ground deformation related to dike intrusion or eruptive fissure opening), though the eruption itself was characterised by sustained gas emission and volcanic tremor during throughout (Neri et al., 2006).

Manchester retrieval: The UMAN team used the iFit approach (Esse et al. 2020) in which a high-resolution solar reference spectrum is used in place of the measured reference more commonly used in DOAS analysis and the fit is applied in intensity space rather than optical depth. In this case, the fit included a SO_2 spectrum (295K, Rufus et al. 2003), two O_3 spectra (223K and 293K; Voigt, 2001), a Ring spectrum, a third order background polynomial, a flat intensity offset and a wavelength shift and squeeze. Finally, the instrument line shape (or slit function) was modelled as a super-Gaussian function (Beirle et al. 2017) with the four defining parameters (FWEM, k, a_w and a_k) fitted alongside the other parameters.

INGV-OE retrieval: Spectra were evaluated following the DOAS method (e.g., Platt et al 2008) from the spectra within the optimal fitting window 307.5–320.0 nm found by obtaining near random fit residual structures with minimal standard deviation and using high-resolution absorption cross sections for SO_2 and O_3 and the Ring spectrum [e.g., Vandaele et al., 1994; Malicet et al., 1995; Chance, 1998]. The time- and position-stamped SO_2 column amounts were integrated along a perpendicular transect to the plume (i.e., wind) direction to yield a cross-sectional amount, which was then multiplied by the wind speed to estimate the SO_2 flux.

Figure 1 displays our comparison between the column amounts (CA) obtained by INGV-OE and those of UMAN. There is a strong linear correlation (R^2 = 0.99, slope = 1.02-1.03) between the data sets. Similarly, strong agreement is evident in Figure 2, where we compare the calculated SO_2 mass flux from each team. The flux for each traverse was calculated using a wind speed of 5 ms^{-1} (Table 1). As with the column amounts, the calculated fluxes agree almost exactly, with only the first not within calculated uncertainty. The error affecting SO_2 flux measurements has been widely discussed since the first application of COSPEC in the late 1980s. The uncertainty is mainly due to the error in wind-speed measurements but also the uncertainty on the estimation of the plume height and the different wind speed inside the plume, even if the latter can affect significantly the flux estimate only under cases of severe wind shear (Hoff and Millan, 1981). Malinconico (1987) estimated the uncertainty at high altitudes to be 15 to 25 %, which agrees with that of 20 - 30% reported SO_2 flux values by Stoiber et al. (1983), Caltabiano et al. (1994) and Mather et al. (2006). Salerno et al. (2009) estimated the overall budget error of SO_2 flux by scanning stationary automatic scanning array considering the individual error of column amount retrieval, multiple scattering, wind-speed, plume height and inversion of flux from slant column amounts between −22 and +36%. This is comparable with the −20 and+36% estimated by Edmonds et al. (2003a) and Arellano et al. (2008), and with ±15–50% evaluated by McGonigle et al. (2003). The overall strong agreement between the column amounts is encouraging, despite the potentially larger uncertainty that errors in the wind field could impose. We also note that further systematic errors are possible, e.g., issues from non-ideal radiative transfer such as a light dilution or optically thick plumes. Under the circumstances when these data were collected, we deem light dilution to be of limited significance since the measurements were made so close to the plume (by helicopter traverse). The potential impact of multiple scattering is much harder to define without extensive radiative transfer modelling (e.g., Kern et al., 2012; 2013).
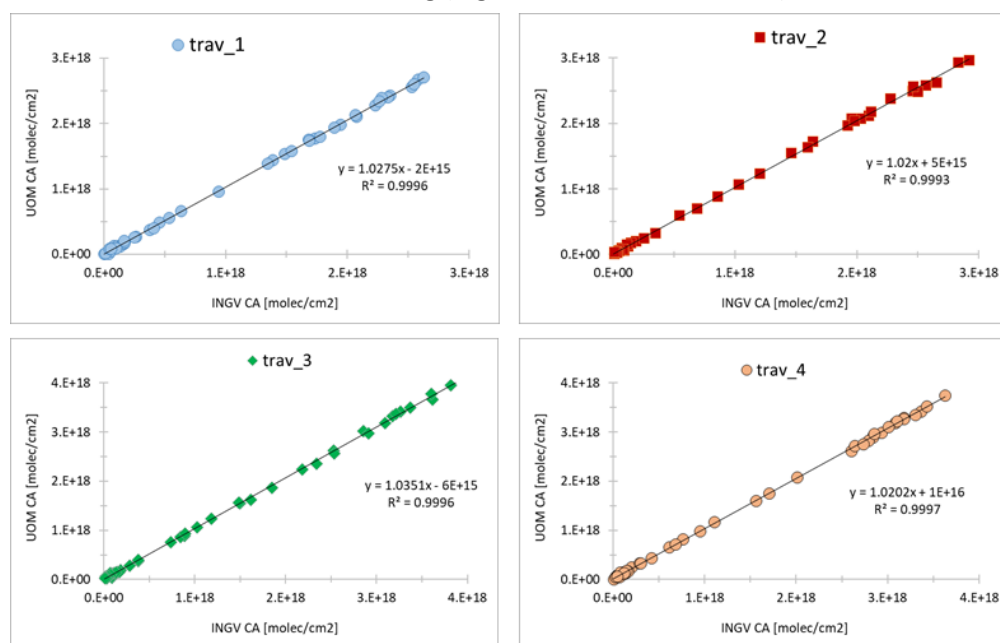

Figure 1: *Comparison of column amounts obtained by INGV and UOM. For each traverse, the correlation coefficient exceeds 0.99 indicating strong correlation. The range in slope is small (1.02-1.03). All traverses were made on the same day in July 2006.*

Table 1: Summary of SO2 flux estimates made by the UMAN and INGV-OE teams

Traverse Number	SO$_2$ Flux [kg/s]		Percent Difference (%)
	UMAN	INGV	
1	60	53	12.3
2	53	52	1.9
3	75	73	2.7
4	57	56	1.8
Average	61	58	5.0
Stdev	10	10	-
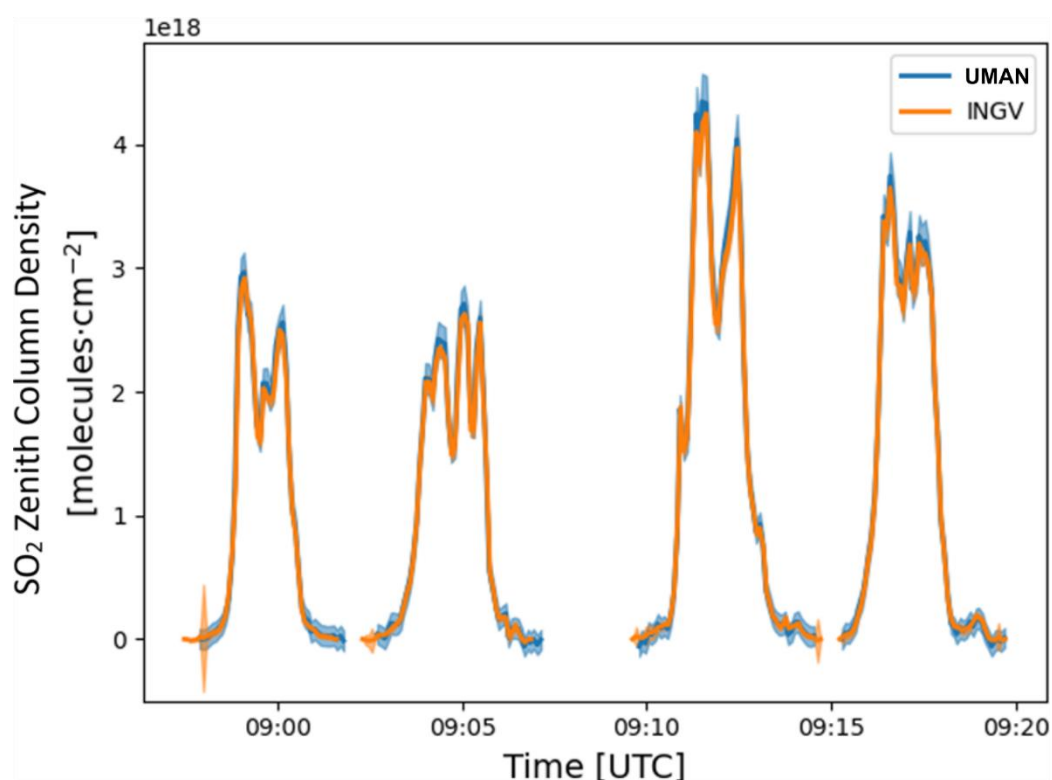
Figure 2. *Comparison of SO$_2$ column densities retrieved by University of Manchester (UMAN) and INGV Osservatorio Etneo (INGV-OE) during 4 scans of the 2006 Etna eruptive plume. Errors are shown by the shading around the lines.*

Finally, we note that it is possible wider discrepancies could have arisen between the column amounts and flux estimates of different groups, had we been able to conduct fieldwork together. Using different instruments, even simultaneously, we might anticipate divergent results owing to differences in spectrometer characteristics, optical collimator configuration and field of view, the fitting windows used in the respective retrievals, or whether clear-sky spectra and dark are measured or modelled. Evaluating these differences in detail cannot be done without multi-team fieldwork and must remain the focus of future work.

3b. Plume composition – Etna & Stromboli

These data were provided by INGV-PA and have been studied by CIVISA, INGV-PA, IMO, and IPGP-OVSG. The data provided comprise three sets of MultiGAS measurements acquired from a single instrument deployed close to the active summit vents. The Etna data was obtained on 3rd June 2010, during a relatively quiet period of activity.

Table 2: *Details of the instrument configuration of the MultiGAS sensors used in this study.*

	Target Gas	Type	Range (ppm)	Resolution (ppmv)	Date last calibration	Syringe present	Filter present
IPGP-OVSG	H_2S	City Tech Electrochemical Type 2E	0-200	0.7	11/02/19	No	Yes
	SO_2	City Tech Electrochemical Type ST/F	0-50	0.1	11/02/19		
	H_2	City Tech Electrochemical Type EZT3HYT	0-200	0.5	11/02/19		
	CO_2	Gascard IR spectrometer	0-3000	0.8	11/02/19		
	H_2O	Galtec RH sensor	0-100 %	-	11/02/19		
INGV-PA	H_2S	City Tech Electrochemical Type 2E	0-50	0.7	07/02/19	Yes	Yes
	SO_2	City Tech Electrochemical Type ST/F	0-200	0.1	07/02/19		
	H_2	City Tech Electrochemical Type EZT3HYT	0-200	0.5	07/02/19		
	CO_2	Licor 840A	0-5000	0.3	07/02/19		
	H_2O	Licor 840A	0-60000	3.7	07/02/19		
CIVISA	H_2S	T3H CitTicel (CTL)	0-50	0.25	12/02/18	Yes	Yes
	SO_2	3MSTF CiTicel (CTL)	0-200	0.5	12/02/18		
	H_2	T3HYT CiTicel (CTL)	0-200	2	12/02/18		
	CO_2	OEM Gascard NG IR spectrometer	0-3000	*not reported*	12/02/18		
	H_2O	Mela thermohygrometer	0-100 %	*not reported*	12/02/18		
IMO	H_2S	City Tech Electrochemical Type 2E	0-50	*not reported*	15/10/18	Yes	Yes
	SO_2	City Tech Electrochemical Type ST/F	0-50	*not reported*	15/10/18		
	H_2	*malfunctioned*	n/a	*not reported*	15/10/18		
	CO_2	Gascard IR spectrometer	0-3000	*not reported*	15/10/18		
	H_2O	*not reported*	0-100 %	*not reported*	15/10/18		

The previous eruption of Etna was an effusive eruption that lasted from May 2008 to July 2009, and was followed by an interval of mostly passive degassing from the summit craters and, after November 2009,

Strombolian activity centred on a small pit at the base of the South East Crater (Global Volcanism Program, 2012). Shortly after our data were acquired, notable events at the volcano include a collapse of the small pit crater on 19 June and powerful explosions from Bocca Nuova during July and August 2010.

Figure 3. *Google Earth illustrations of Stromboli (left) and Etna (right) with approximate locations of MultiGAS instruments shown by yellow stars.*
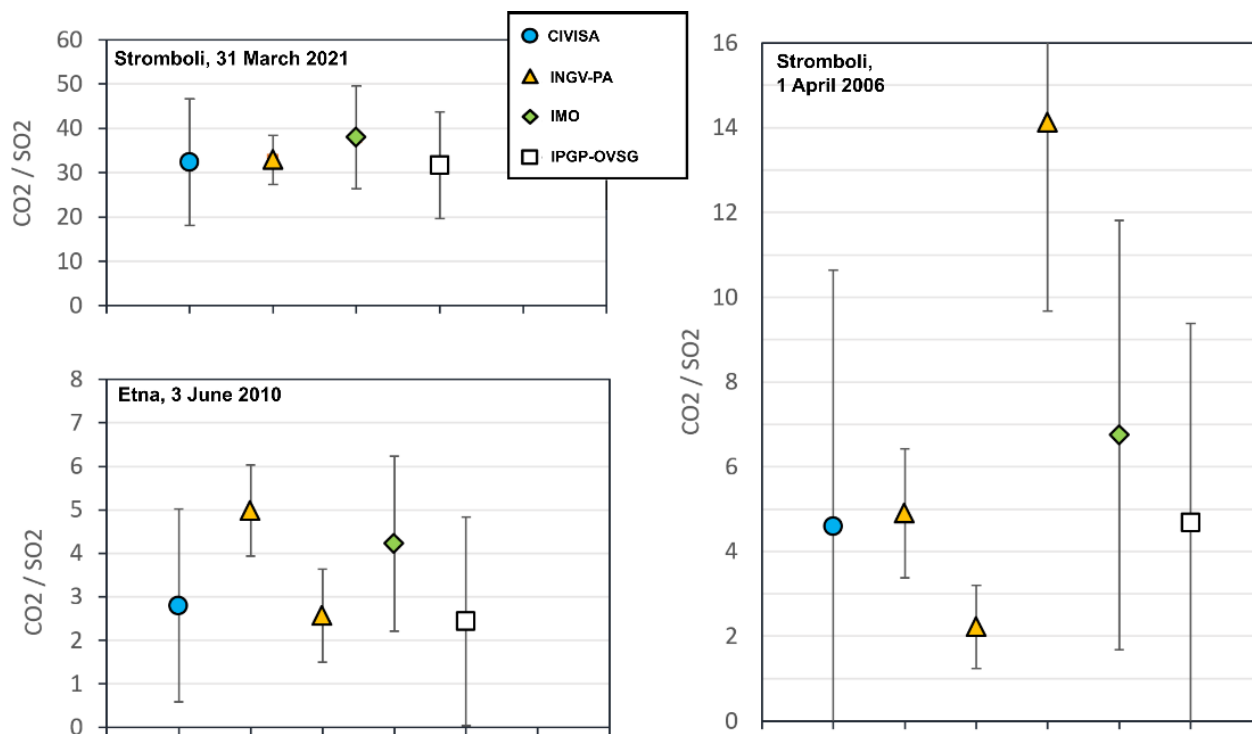

Figure 4. *CO_2/SO_2 ratios obtained by each group for three days of activity at Etna and Stromboli, based on measurements obtained by INGV-Palermo (INGV-PA) MultiGAS instruments.*

Our first Stromboli data set dates from April 2006, an interval of quiescence on the volcano prior to the major flank eruption of Febuary-March 2007 (Global Volcanism Program, 2007). Our second data set is from March 2021, another period of typical Stromboli behaviour, that is, ongoing Strombolian eruptions and stable SO_2 emissions of around 250-300 t/d (Global Volcanism Program, 2021). The instruments deployed on each volcano are of standard INGV construction. The configuration of these and the other MultiGAS instruments referred to in the following sections are reported in Table 2.

Etna. INGV Palermo calculates two separate estimates of CO_2/SO_2, representing different intervals of the data acquisition window. CIVISA, IMO and OVSG all choose longer intervals for their ratio estimates, spanning more of the acquisition window in each case. The closest agreement between groups is that between CIVISA and OVSG, resulting from similar window lengths. As shown in Figure 4, however, these ratios are subject to much larger errors than either of the INGV Palermo estimates. The selection of shorter windows here results in improved correlation between CO_2 and SO_2, but care must be taken not to eliminate too much data by adopting too short a window (see Discussion below). It is likely that these different estimates of CO_2/SO_2 result from fluctuations in gas chemistry on timescales shorter than the acquisition period (~20 minutes) but longer than the INGV window lengths (~5-10 minutes). This illustrates how selection of window length can dramatically influence the CO_2/SO_2 ratio obtained. For monitoring purposes, where high-frequency fluctuations in gas composition may be important to identify, shorter window lengths might be advantageous, as opposed to scenarios when we attempt to characterise the overall or 'background' composition of a volcano's gas emissions, where longer acquisition windows are important to average out short-term variability.

Table 3: *Summary of CO2/SO2 ratio and related parameters based on each group's analysis of data provided by INGV Palermo, obtained by MultiGAS measurements on the summit of Etna on 3rd June 2010.*

Etna 03/06/10	CO_2/SO_2	Error (±)	R^2	Filter applied?	Window length	No. points	Max SO_2 (ppm)
CIVISA	2.8	2.22	0.53	Shift: 0/0	13:16-13:35	121	26.1
INGV	4.98	1.05	0.79	none	13:18-13:30		19.8
INGV	2.57	1.07	0.81	none	13:30-13:35		26.3
IMO	4.22	2.01	0.93	none	13:18-13:25		20
OVSG	2.44	2.40	0.63	none	13:18-13:35	110	26

Table 4: *Summary of CO2/SO2 ratio and related parameters based on each group's analysis of data provided by INGV Palermo, obtained by MultiGAS measurements on the summit of Stromboli on 31st March 2021.*

Stromboli 31/03/21	CO_2/SO_2	Error (±)	R^2	Filter applied?	Window length	No. points	Max SO_2 (ppm)
CIVISA	32.4	14.25	0.78	Shift 0/-1	18:09-18:27	124	0.9
INGV	32.89	5.57	0.81	Shift 0/-2	18:09-18:25		0.9
IMO	37.98	11.60	0.93	Shift 2, Filter 4, Filter 2	18:09-18:22		0.8
OVSG	31.71	12.00	0.89	Shift 1	18:09-18:29	138	0.9

Table 5: *Summary of CO2/SO2 ratio and related parameters based on each group's analysis of data provided by INGV Palermo, obtained by MultiGAS measurements on the summit of Stromboli on 1st April 2006.*

Stromboli 01/04/06	CO_2/SO_2	Error (±)	R^2	Filter applied?	Window length	No. points	Max SO_2 (ppm)
CIVISA	4.6	6.04	0.26	Shift: 0/0	00:01-00:21	138	16
INGV	4.9	1.52	0.61	Median 3/3	00:00-00:14		13.6
INGV	2.22	0.99	0.88	Shift 0/-1	00:16-00:18		15.96
INGV	14.13	4.46	0.75	none	00:20-00:27		10.19
IMO	6.75	5.06	0.63	Filter 5	00:05-00:20		12
OVSG	4.68	4.70	0.69	Shift 1	00:05-00:20	103	16

Stromboli. All four CO_2/SO_2 estimates on 31st March 2021 fall in the range of 32-38, albeit with large errors. The window lengths are broadly similar in each case, though each group adopted differences in filtering and time shifting. We imposed no control on the choice of filters or time shifts, leaving this open to the interpretation of each group. The large errors may be a result of low SO_2 concentrations (< 1ppm), contributing to wide ranges in CO_2/SO_2 across the data set. The correlation coefficients on each ratio estimate are greater than 0.6. In contrast, the CO_2/SO_2 estimates on 1st April 2006 are spread across a larger range and exhibit proportionally larger errors, in some cases of greater magnitude than the ratio itself. The CIVISA ratio estimate was calculated from the longest window and has the lowest correlation coefficient. Shortening the window length over which the ratio is calculated improves the correlation, as demonstrated by the other groups, though the choice of window is subjective and open to interpretation. Again, each group adopt different filters and temporal shifts.

3c. Plume composition – Furnas

This is a contrasting case, a fumarole-dominated volcano in a state of long-lived quiescence rather than the persistently active open-vent volcanoes of Etna and Stromboli. In practice, this means that the gas compositions measured are further from 'ideal' magmatic compositions due to interaction with a substantial hydrothermal system and that SO_2 is not the dominant sulfur species (rather H_2S). We have a suite of coincident MultiGAS measurements undertaken by CIVISA, INGV-PA, IPGP-OVSG and IMO at four fumaroles (Fig. 5) located at Furnas Village Fumarolic Field (Caldeira Grande, Asmodeu, Pêro Botelho and Esguicho) and two sampling points at Furnas Lake Fumarolic Field (Furnas Lake 1 and Furnas Lake 2). In addition, all four teams (CIVISA, INGV-PA, IPGP-OVSG and IMO) ran their typical post-processing approaches on the INGV-PA dataset from Caldeira Grande. The discussion in this report will be focus on the data of Caldeira Grande fumarole, though for complete reporting we include the measurements across the six sites in Figure 6b and Table 6. We have some further data from the IPGP-OVPF group on Caldeira Grande that we discuss in relation to the challenges of establishing background concentrations of water and CO_2. The Furnas data were acquired during fieldwork in 2019 in the Azores undertaken as part of Task 5.1. There is therefore a good opportunity here to compare not just the various MultiGAS data sets acquired, but to compare these data to the gas chemistry obtained by lab analysis of gas samples obtained by our Task 5.1 colleagues on Caldeira Seca fumarole located approximately 15 m from Caldeira Grande fumarole.
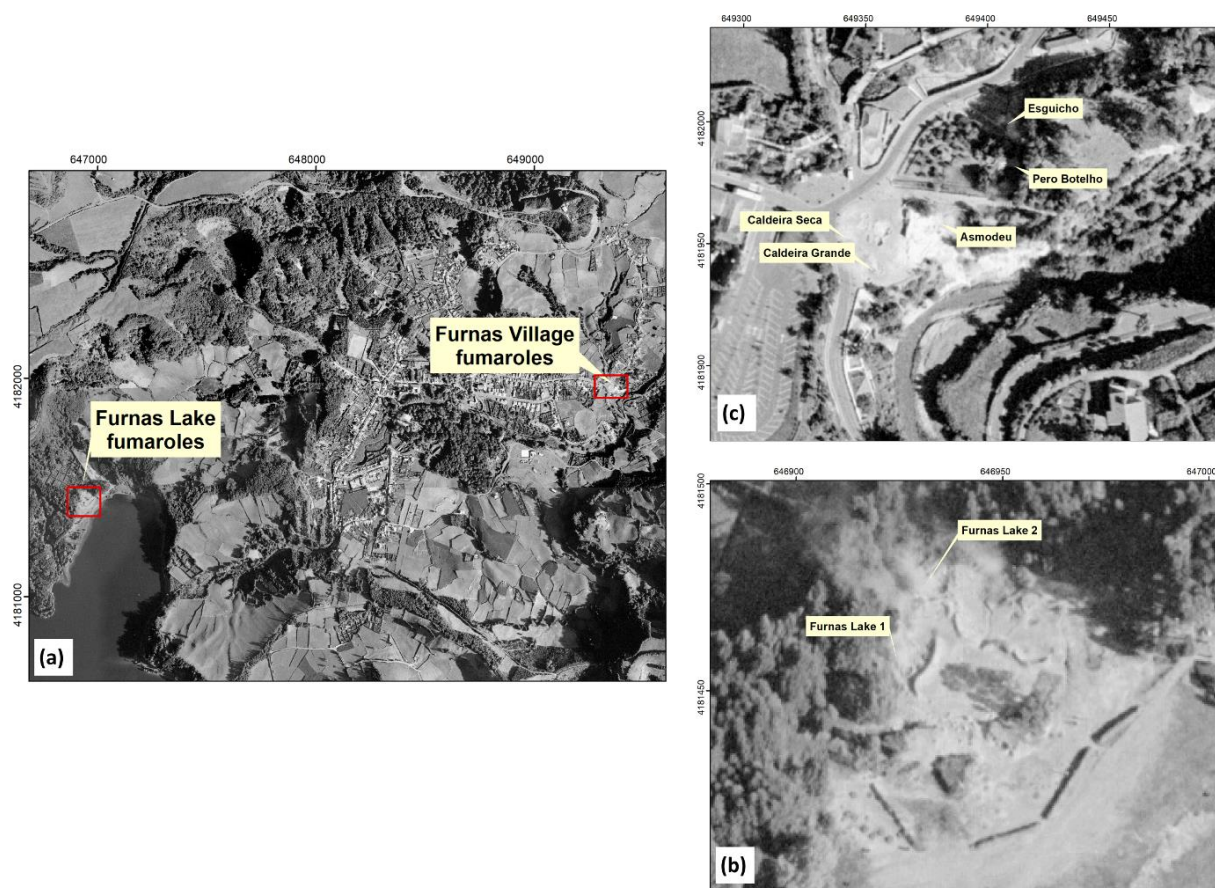
Figure 5. Map of the north part of Furnas volcano caldera with the location of the sampling sites: a) Location of Furnas Lake and Furnas Village fumarolic fields; b) a zoom detail showing the sampling sites at Furnas Lake fumarolic field and c) a zoom detail showing the location of the sampled fumaroles in the Furnas village area. Caldeira Grande is the site of all the MultiGAS data we show herein and Caldeira Seca is the direct sampling site.

Figure 6a (right). *Plume composition ratios obtained from Caldeira Grande fumarole (Furnas). Panel (a) shows ratios derived by each listed team from their own MultiGAS measurements, made on 21 February 2019. Panel (b) and (c) correspond to re-analysis of the INGV-Palermo data by each listed team.*
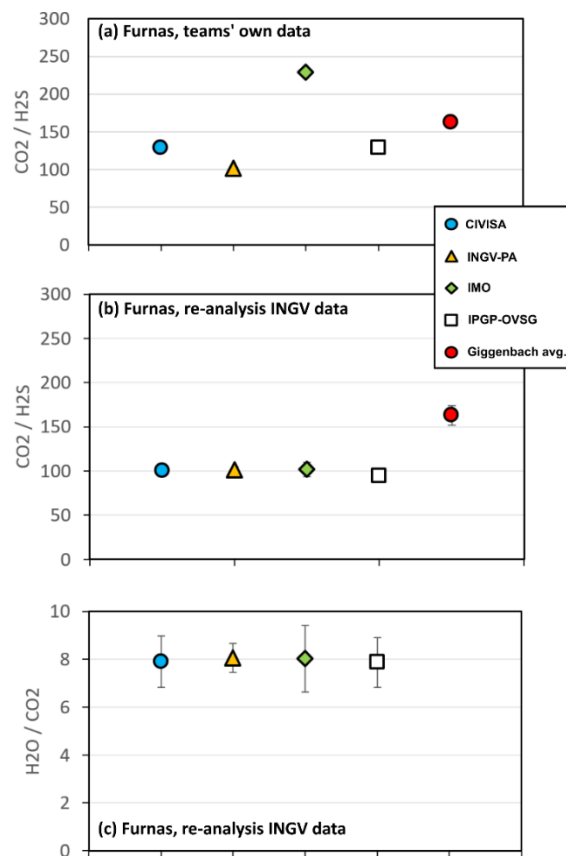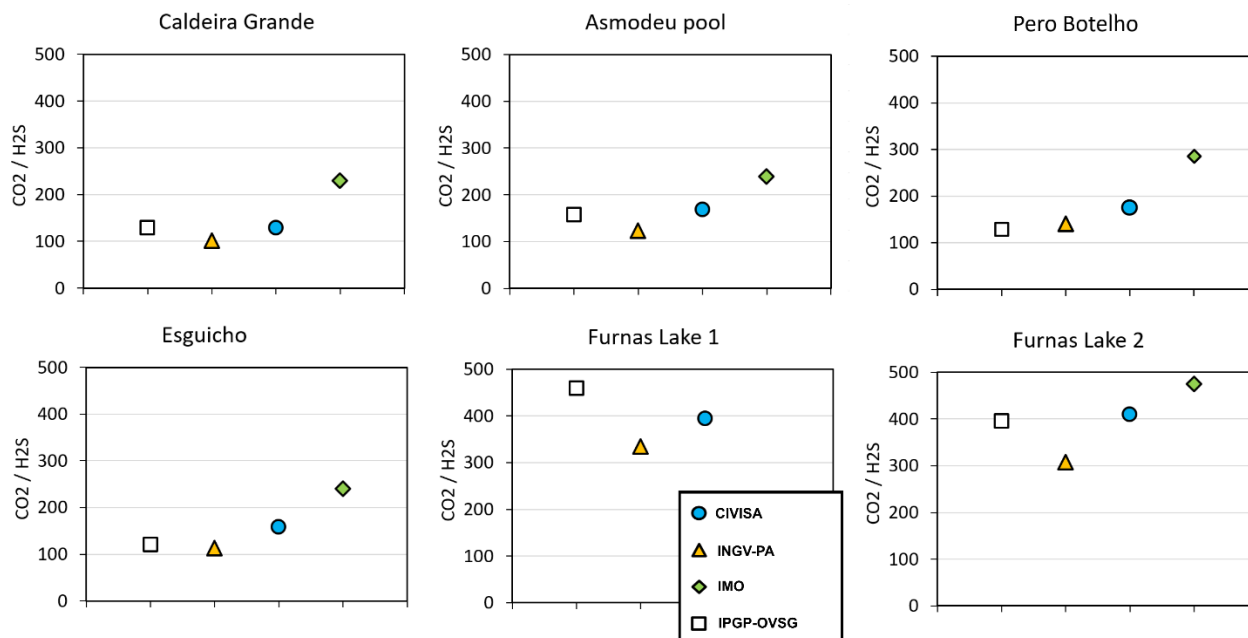

Figure 6b (below). *Plume composition ratios obtained from six sites across Furnas caldera (see map in Figure 5). Our discussion in this report focusses on Caldeira Grande, though we note that there is generally good agreement between the CIVISA, INGV and IPGP measurements of CO_2/H_2S, with IMO consistently deriving higher ratio.*

In Figure 6a, we show in the upper panel the CO_2/H_2S molar ratio derived from independent MultiGAS measurements made by each team during the Azores field campaign. All the data shown in this Figure correspond to measurements made at the Caldeira Grande site. Alongside the MultiGAS data, we plot the mean CO_2/H_2S obtained from laboratory analysis of gas samples acquired by the Giggenbach methodology at Caldeira Seca Fumarole, located about 15 m from Caldeira Grande fumarole (Caldeira Grande is no longer sampled by CIVISA, for safety reasons). The CIVISA and IPGP-OVSG ratios agree exactly (= 129), while the INGV-PA (101) and IMO (229) ratios falling either side, with percent difference of -24% and +56% respectively. The ratio obtained from eighteen Giggenbach bottle samples and analysed across four labs is equal to 163, a percent difference of +23% from the CIVISA and OVSG ratio. The IMO data is a clear outlier, and the correlation on the ratio is lower than those of the other groups (Table 6).

In panel (b) we show the CO_2/H_2S ratios obtained when each group subjects the INGV-PA measurements to their own post-processing, while panel (c) illustrates the corresponding H_2O/CO_2 ratios. The range in CO_2/H_2S is significantly narrower, from 94-102 (+8% percent difference), and the H2O/CO2 ratios range from 7.9-8.1, albeit with errors up to 12%. This improved agreement between the four estimates of CO_2/H_2S may illustrate that differences in post-processing alone are not the source of the range in ratios plotted in panel (a), contrasting with the arguments outlined above for Stromboli and Etna. The divergent estimates of plume composition shown in panel (a) may be a consequence of different window lengths, with the IMO acquisition being half the length of the others.

Comparison with data from Giggenbach bottles
For high temperature fumaroles (>250°C), MultiGAS measurements have been shown to closely match analyses of direct fumarole sampling via Giggenbach bottles (Aiuppa et al., 2005; 2007). For low-temperature fumaroles (100 °C), despite some minor offset due to secondary phenomena, such as gas scrubbing from water droplets in air and diffusive-effusive gradients in the MultiGAS sampling line imposed by both the inlet filter and pump, results from both techniques showed good coherence (Moretti et al., 2020).

In case of our Furnas data, four teams measured the CO_2/H_2S of low-temperature fumaroles of Furnas with Giggenbach bottles, at the Caldeira Seca emission site. Eighteen samples gave an average CO_2/H_2S ratio of 163 ± 11 (*see Report Task 5.1*). This falls close to the range of the CO_2/H_2S ratios obtained from our MultiGAS measurements (range: 101 to 229; average: 127 ± 56, included an outlier (229, IMO) or range: 101 to 129; average 120 ± 16) with a positive shift evident in the values obtained from the direct sampling. An offset between direct sampling and in situ measurements by MultiGAS has been observed at other volcanoes (i.e., La Soufrière de Guadeloupe; Moretti et al., 2020) and could be minimized in periods of increased vent emission rates (Moune et al., submitted to Frontiers). Moreover, the differences could also result from the fact that, despite the proximity of the sample sites (MultiGAS vs direct sampling), the sampling was performed in two different fumaroles. However, the CIVISA team performed an extra survey on the 24th of September 2020, where Caldeira Seca was sampled with both MultiGAS and Giggenbach bottles and the CO_2/H_2S ratios in this survey were 168 for the Giggenbach methodology and 163 for the MultiGAS. Overall, our combined dataset shows a good agreement between these two techniques and gives us confidence that the MultiGAS approach can provide a valid means to survey gas composition at low temperature fumarolic systems, especially given the lack of advanced analytical labs close to many volcano observatories worldwide.

Table 6: This table reports the CO2/H2S ratios obtained by each group's own MultiGAS measurements undertaken in Caldeira Grande Fumarole (Furnas) during the Task 5.1 field campaign.

Furnas 21/02/19	CO_2/H_2S	R^2	Window length	Max H_2S (ppm)
Caldeira Grande				
IPGP-OVSG	*129*	*0.98*	*11:49-12:45*	*18*
INGV-PA	*101*	*0.86*	*11:49-12:45*	*18*
CIVISA	*129*	*0.82*	*11:49-12:45*	*11.7*
IMO	*229*	*0.74*	*12:26-12:49*	*14*
Pêro Botelho				
IPGP-OVSG	*129*	*0.74*	*14:31-14:44*	*5*
INGV-PA	*141*	*0.91*	*14:31-14:44*	*14.5*
CIVISA	*176*	*0.97*	*14:31-14:44*	*7.6*
IMO	*285*	*0.87*	*14:30-14:44*	*6*
Esguicho				
IPGP-OVSG	*120*	*0.76*	*14:45-15:09*	*6*
INGV-PA	*112*	*0.84*	*14:45-15:09*	*10*
CIVISA	*158*	*0.96*	*14:45-15:09*	*7.6*
IMO	*240*	*0.87*	*14:47-15:01*	*4.5*
Asmodeu Pool				
IPGP-OVSG	*157*	*0.96*	*14:02-14:28*	*9*
INGV-PA	*123*	*0.88*	*14:02-14:28*	*12*
CIVISA	*169*	*0.96*	*14:02-14:28*	*11*
IMO	*239*	*0.87*	*14:03-14:24*	*8*
Furnas Lake 1				
IPGP-OVSG	*459*	*0.97*	*13:16-13:26*	*2*
INGV-PA	*334*	*0.90*	*13:16-13:26*	*2.4*
CIVISA	*394*	*0.84*	*13:16-13:26*	*0.95*
IMO	*-*	*-*	*-*	*-*
Furnas Lake 2				
IPGP-OVSG	*395*	*0.97*	*12:50-13:14*	*2*
INGV-PA	*334*	*0.90*	*12:50-13:14*	*2.6*
CIVISA	*410*	*0.97*	*12:50-13:14*	*2.1*
IMO	*475*	*0.65*	*13:00-13:13*	*2.5*

Furnas 21/02/19	CO_2/H_2S	H_2O/CO_2	Error (±)	R^2	Filter applied?	Window length	Max H_2S (ppm)
CIVISA	100.3		5.97	0.83	Shift 0/-1	12:55-13:56	17.4
		7.9	1.07	0.56	Shift 10/-10	13:04-13:51	17.4
INGV	101.0		3.70	0.86	Shift -4	13:27-13:52	17.4
		8.1	0.60	0.65	Median 1/4 Shift 7/-10	13:26-13:46	
IMO	101.8		8.29	0.89	Shift -4 Filter 7	13:26-13:46	18.0
		8.0	1.39	0.65	Shift 16	13:26-13:46	
OVSG	94.5		6.81	0.76	none	13:07-13:58	17.0
		7.9	1.04	0.49	Shift 10	13:07-13:58	

Table 7. *This table reports the CO_2/H_2S and H_2O/CO_2 ratios obtained by each group's re-analysis of the INGV-PA measurements at Caldeira Grande fumarole (Furnas).*
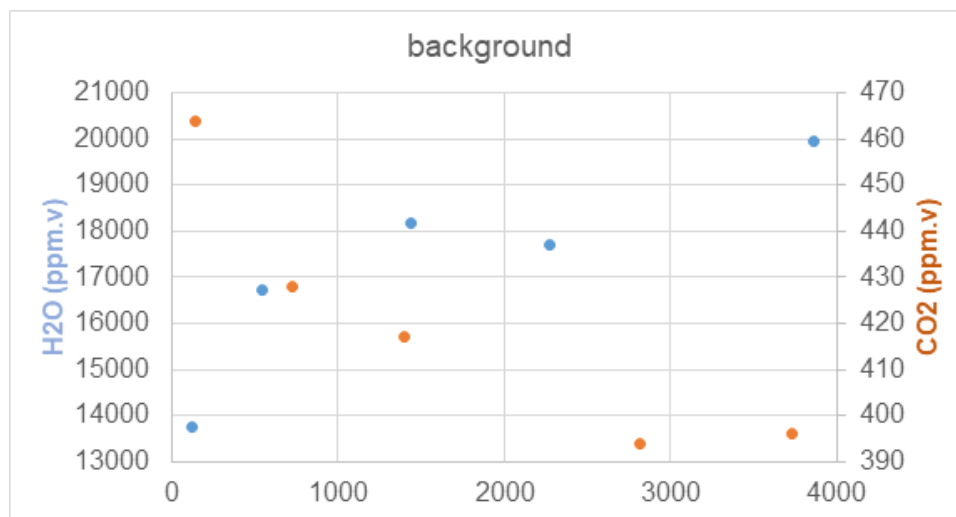

Figure 7. *Time series (x-axis, seconds) of MultiGAS (IPGP-OVPF) H_2O and CO_2 concentration notionally made away from the Caldeira Grande fumaroles (averageH2S concentration 1.6 ppmv; range 0.1-6.9 ppmv), the location used for Task 5.1. The CO_2 and H_2O concentration are clearly not constant throughout the sampling interval.*

4. Discussion

The preceding section illustrates that significant variation in estimated plume composition (i.e., molar abundance ratios, e.g., CO_2/SO_2, CO_2/H_2S) can arise when different post-processing approaches are applied to simultaneously acquired measurements. Perhaps counter-intuitively, our results show a suite of MultiGAS instruments placed in the same plume (Furnas) yielding plume composition estimates in good agreement, while different post-processing approaches to the same set of measurements (acquired from single instruments on Etna & Stromboli) yield divergent compositions. In the following section we briefly explore selected elements of both analysis and post-processing to elaborate the potential source of these discrepancies.

Evaluation of background gas concentrations

A critical early step in evaluating gas ratios from MultiGAS concentration time series is to first extract, or otherwise correct for, atmospheric background concentrations of the gas species of interest. For sulfur-bearing species like SO_2 and H_2S, this is usually straightforward, since the concentration of these in the background atmosphere is significantly lower than in volcanic plumes (provided measurements are made far from sources of anthropogenic pollution). For water and CO_2, it is far more challenging since both are abundant in the ambient atmosphere. The principal implication for this is in accurate derivation of the

H_2O/CO_2 ratio. Normally gas ratios are derived from linear regression of the concentrations of each component referred to H_2S or SO_2, these latter being of purely volcanic origin. Such a simple procedure does not require any correction for the atmospheric background in case of CO_2 and H_2O, which are both volcanic and atmospheric components

The background concentration can be either (i) identified via the regression line of the CO_2/SO_2 correlation, or (ii) obtained from a series of measurements performed with the MultiGAS outside the region of volcanic gas plume influence. Use of the regression line is simple, with the intercept of the regression line with the graph's vertical axis indicating the value of the local background. Where background values are anomalously high, e.g., $CO_2 \gg 400$ ppm, this may be an indication of volcanic gases contaminating the background signal, whether from advection of a crater plume or mixing with diffuse gases rising through the soil. In such circumstances, MultiGAS concentration datasets must be assumed to be compromised, and monitoring of concentrations unambiguously outside the plume must be adopted in order to quantify background concentrations accurately. Figure 7 illustrates the potential challenges involved in defining background concentrations based on direct measurements.

This prompts the question of which value is the most suitable for selection of a background concentration for each species. Frequently used approaches fit the atmospheric CO_2 background to the local minima of the time series. The adoption of such an approach to treat the Azores time series would result of a change in CO_2 atmospheric background of up to 70ppm.v, an amount much larger than the full expected daily variability (< 5-10 ppm.v). In the data treatment, we could thus prefer to fit a linear baseline to the lowest values of the CO_2 background (ca. 400 ppm.v), whose values are closer to the expected standard air CO_2. This choice implies that the apparent background of the early measured data is affected by a locally high CO_2 flux and cannot be considered equivalent to the CO_2 background outside the plume. In the case of water, the choice of the background is ever trickier. If we consider that the first data recorded have a larger plume contribution (higher CO_2), the atmosphere of this area has also the lower H_2O concentration.

The "fitting the minima" procedure would imply an enormous range in background atmosphere vapor water, which is inconsistent with the little changing pressure and temperature conditions during the time interval of the measurement. For the treatment of water, we thus choose again to keep a straight background passing for the lowest point; interestingly, a similar increase in background is found in H_2S data, which show a global correlation with H_2O data.

A consequence of this line of reasoning is that the definition of the background is much more robust when an extended dataset well outside the plume area is recorded. For monitoring purposes, one could imagine a separate station being installed away from plume influence that provides continuously updated records of atmospheric chemistry and conditions, though in resource-poor settings this may not be tractable and regular deployments of a MultiGAS in non-plume settings to evaluate fluctuations in background concentrations (e.g., seasonality) may be sufficient.

Choice of regression method

We tested two different regression methods on the Etna and Stromboli data (see red and blue straight lines in following Figure 8, Figure 9): the commonly used least-square method (L2; e.g., RatioCalc; Tamburello et al., 2015) and the least-absolute difference method (L1). Both methods were found to yield similar ratios, even though the latter method is known to be less sensitive to outliers (Bloomfield and Steiger, 1983; Dodge, 1997) and could give less associated errors. While this analysis suggests that choice of linear regression is not the most influential control on molar ratios, we consider it a valuable and simple test to incorporate into all post-processing workflows, using two or three methods of fitting a line between two gas concentration data sets and selecting the method that provides the lowest error.

Time-window selection & number of points

The previous section illustrates that the choice of window length over which a molar ratio is calculated can impart a considerable influence on the outcome of the ratio. Attempting to calculate ratios over the full period of data acquisition can yield ratios subject to extremely large errors, due to differential (non-conservative) advective transport of plume gases or periods otherwise characterised by poor correlation between the concentration of multiple species. Therefore, many workers choose to examine the concentration time series derived from MultiGAS measurements and select temporal windows over which the ratios can be better calculated. Often, these windows are selected according to the following criteria:

- Clear peaks in SO_2 or H_2S, which due to low concentrations in the background atmosphere, are less ambiguous signatures of volcanic or hydrothermal plume gases than water or CO_2.
- Durations that comfortably exceed the maximum t90 of any of the gas sensors, in order to ensure that any concentration peak has been adequately resolved.
- Ideally, durations that incorporate multiple concentration peaks, allowing for some of the volcanic system's natural variability to be accounted for.

In this section, we have explored the influence of varying time window length on the retrieved ratios. In Figure 8 and Figure 9, corresponding to Etna and Stromboli, we can see consistently that a lack of correlation between CO_2 and SO_2 when the full data set is used gives way to improved correlation between the species for an adjusted (i.e., shorter) window length. This is indicated by the increase in the correlation

coefficient as well as the decrease in the relative magnitude of the error on the CO_2/SO_2 ratio. However, we can clearly see that the window length adjustment alone is not a sufficient improvement. In Figure 8b, the data is still not well fitted by the two (L2, L1) regression lines shown, and arguably the dashed black lines (drawn, not calculated) would offer improved fit and thus more "correct" ratios. This perfectly illustrates one of the key challenges facing interpretation of MultiGAS data in terms of molar concentration ratios. To achieve ratios with low errors and high correlation between the gas species, we often pursue shorter and shorter window lengths over which to calculate our ratios. However, this yields ratios that only 'fit' short periods of our data acquisition window and do not, therefore, adequately reflect the variability of the plume composition. Figure 9 demonstrates the same process for the Stromboli data. Under many circumstances, it may be more correct to quantify a series of ratios and report the variability, rather than attempting to reduce the complex variation down to a single "representative" value. The calculation of ratios often includes subjective decisions to be made about the correct window length, and we advise that deriving these ratios is based on a balance between window length, number of data points, relative error magnitude, correlation coefficient, and the general variability or stability of the ratios that can be derived in any single acquisition period.

In Figure 10, we illustrate this further by demonstrating how improvements in correlation between CO_2 and SO_2 can be achieved via temporal averaging, taking the mean CO_2 and SO_2 concentration every 60 seconds, and obtaining a ratio from the correlation between these temporally averaged data. However, the data sets are now much smaller and become subject once more to large errors on the ratios. This illustrates the fact that we should not focus solely on correlation between species but must adopt a more informed approach to evaluate the plume composition. A large sample size is required to make the best use of statistical relationships. In practical terms, this means more continuous data acquisition over a longer time interval (<1 day) and calculating a range of ratios over multiple window lengths to evaluate the variability of the apparent signal obtained by MultiGAS.
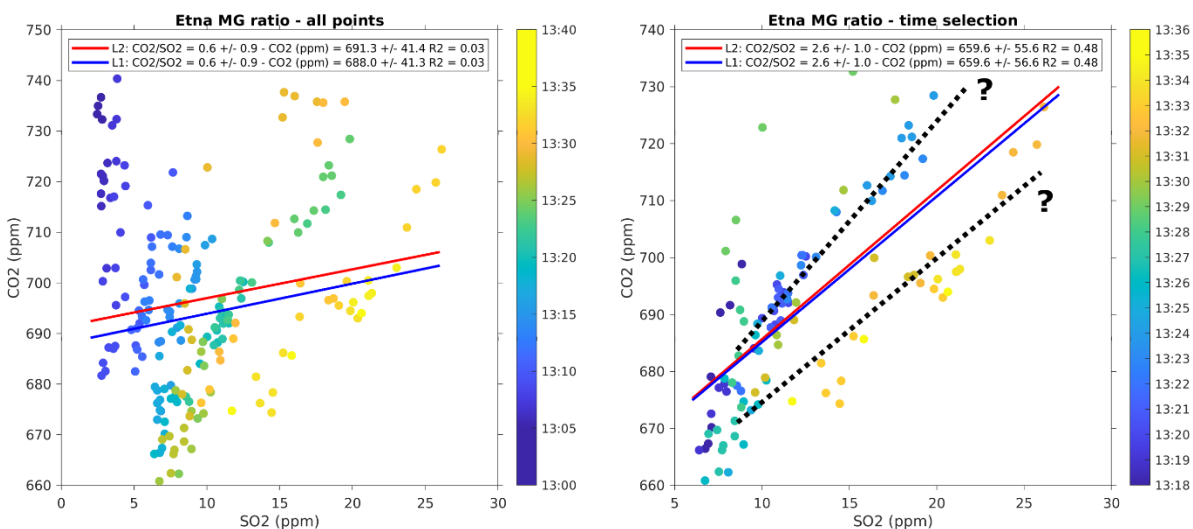

Figure 8. *Treatment of MultiGAS data from Etna, to illustrates the difference in window length. The left plot shows the full MultiGAS data set, i.e. An acquisition interval of around 40 minutes. The right plot shows how changing the window length (shortened to 18 minutes) improves the relative magnitude of the error on the CO_2/SO_2 and the correlation coefficient, with a major concomitant change on the ratio itself, from $CO_2/SO_2 = 0.6$ to $CO_2/SO_2 = 2.6$.*

Note too that the correlation coefficient remains low and that the data could arguably be better fit with two separate lines, each corresponding to shorter windows of around 6-7 minutes, shown by the black dotted lines.
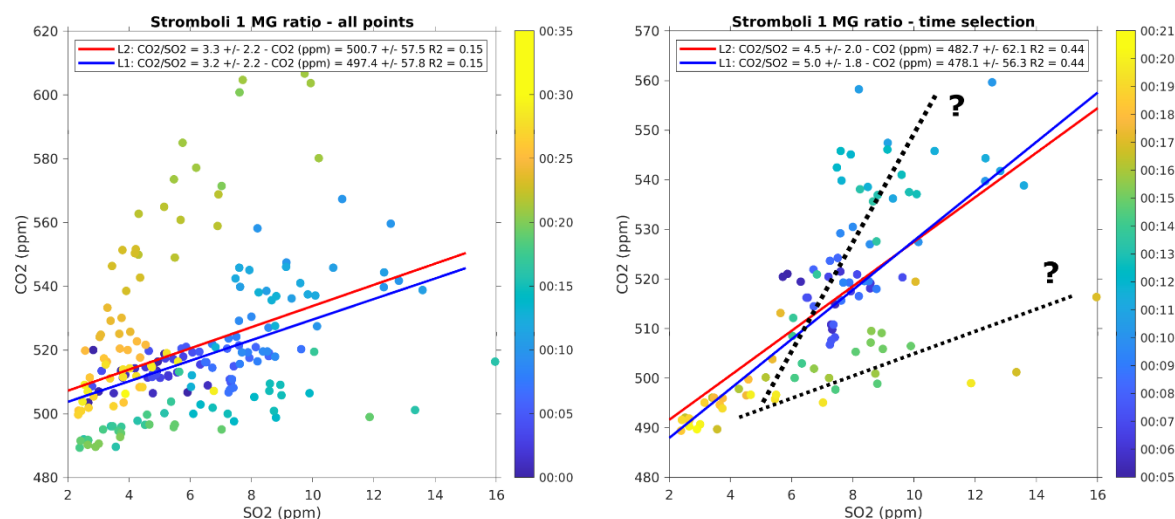

Figure 9. *Treatment of MultiGAS data from Stromboli (2006 campaign), again illustrating that large changes in CO_2/SO_2 ratio result from reducing the length of window over which the ratio is derived, here from 35 minutes to 16 minutes. Note the improvement in correlation coefficient and the reduction in error magnitude. As in Figure 8, however, the regression line in the right hand (modified window) panel does not fit a substantial number of the points, and the derived ratio is therefore still a flawed representation of the true plume composition during this acquisition period.*
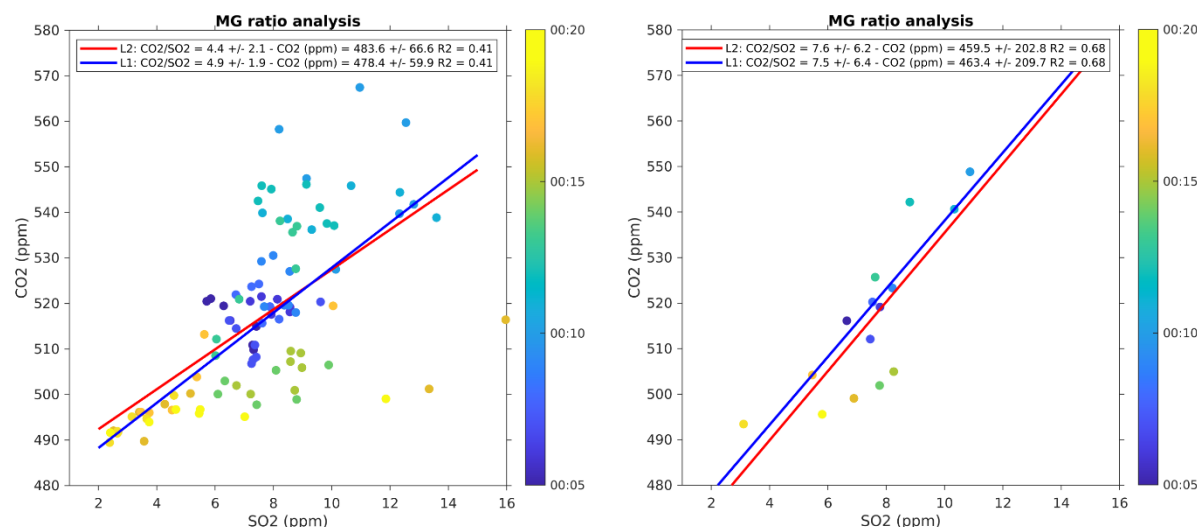

Figure 10. *Treatment of the Stromboli 2006 MultiGAS data, exploring the influence of time averaging to improve the correlation between CO_2 and SO_2. The left panel shows the Stromboli 2006 data, subjected to a shortened window (~20 minutes) and the right panel shows the same data with SO_2 and CO_2 concentrations averaged every 60 seconds. We can see only significant improvement in the correlation coefficient (from 0.41 to 0.68) but suggest that this is of limited real value since (a) the regression is based on many fewer data points and (b) the ratio is subject to much larger uncertainty. We include this Figure principally to illustrate the counterargument to*

shortening the window length for improvements in correlation – a consequence of smaller data sets is an increase in uncertainty/error on the key quantity of interest, namely the CO_2/SO_2 molar ratio.

5. Recommendation of best practices

In the following section, we summarise the main recommendations for best practices for both UV remote sensing of SO_2 flux and in situ measurements of plume composition by MultiGAS, based on discussions undertaken by the Task 5.2 workers and summarising the content of the foregoing report.

5a. Best practices for UV remote sensing of SO_2 flux

- The exposure of the spectrometer (combination of integration time and co-adds) needs to be configured depending on (i) how the SO_2 flux traverse is undertaken (e.g., by helicopter, vehicle, or walking); (ii) the distance between the spectrometer and the volcano vent; (iii) the plume width; and (iv) the eruptive state of the targeted volcano.
- The selected combination of integration time and co-adds should ensure intensities of ~80% of maximum bit-depth of the sensor to maximise signal to noise (balanced with sampling frequency) while avoiding saturation in any region of the spectrum. This requires the operator to assess these parameters in real time while undertaking the measurements.
- The telescope should be calibrated to ensure proper collimation and have a wave-cut filter to block visible light to reduce the impact of stray light.
- Depending on the volcano and the width of the volcano plume, traverse times should be shorter/comparable to variations in degassing patterns to avoid being influenced by degassing variations. This will be more straightforward in a monitoring scenario rather than a field campaign to a previously unstudied volcano, where some prior knowledge of the emissions behavior may be available.
- Depending on the volcano, traverses should be made as close to orthogonal to the plume direction as possible.
- A GPS log should be recorded over the entire traverse sampling such as to timestamp the spectra and correct the traverse for the effects of non-orthogonality with respect to the volcanic plume.
- Clear-plume sky and dark spectra should be recorded at the start and end of each traverse.
- Wind speeds should be measured directly if possible at the start and end of the traverse sampling (e.g., using an anemometer or co-deployed SO_2 camera)
- The distance between the instrument and the plume should be a short as possible to minimise light dilution; post-acquisition, spectra should be checked for light dilution impacts and corrected if possible.

5b. Best practices for MultiGAS measurements of plume composition

- All sensors must be regularly calibrated in the laboratory using target gases of known concentration. The t90 behaviour (the time required to reach 90 % of the final signal following a step change in gas abundance) of all sensors should be determined via calibration tests with various gas mixture ratios. The interference of SO_2 on H_2S, a widely reported cross-sensitivity in the electrochemical sensors used in most MultiGAS instruments, should be checked and characterised (e.g. Roberts et al., 2014).
- The MultiGAS should be positioned close to a volcanic vent ensuring the inlet tube is exposed to gas emissions, at 0.5-1 m height above the ground in order to avoid any influence from soil degassing.

Care should be taken not to place the sensor too close to the vent as this can cause condensation buildup or gas sensor saturation.

- The MultiGAS should be placed inside the plume for at least 10 minutes to capture the short-term fluctuation of the plume composition and have also enough points to well-constrain the exact gas composition (see below).
- External sensors should be used for H_2O determination, as they increase the potential of minimising the influence of steam condensation within the MultiGAS inlet tubing. However, it is important to note that in specific conditions (such as water-rich fumarole plumes, tropical environments), the H_2O determination can still be underestimated (up to 40%; Gaudin et al., 2016; Jessop et al., 2021) due to rapid partial steam condensation.
- Diffusive-effusive gradients in the MultiGAS inlet pumping line have been observed inducing chemical modification. We thus suggest to further test/compare MultiGAS measurements with or without pump to well characterise this inlet pumping line effect.
- An extended MultiGAS dataset well outside the plume area is recommended to evaluate fluctuations in background concentrations.
- To minimise residuals, different regression methods should be tested, since some methods are less influenced by outliers. We recommend choosing the regression method that gives the best correlation coefficient. However, as mentioned above, a better correlation coefficient should not be treated as a direct path to a more correct result. It is also important to constrain the associated errors well and consider the correlation coefficient and error in tandem, as joint indicators of robust ratio determinations. To minimise errors, we recommend that acquisition times or window lengths (for ratio calculation) are not shortened too much solely for the purpose of improving the R^2 (see below).
- All gas pulses with a duration shorter than the lowest t90 of the species of the considered ratio are not well-captured by the sensors. A low-pass filter at the lowest t90 should be applied to all measured concentration data in order to overcome this.
- To achieve ratios with low errors and high correlation between the gas species, we recommend shorter window lengths, keeping in mind that low number of data (<100) will induce larger errors. However, a large sample size is required to make the best use of statistical relationships. In practical terms, we suggest more continuous data acquisition over a longer time interval (<1 day) and calculating a range of ratios over multiple window lengths to evaluate the variability of the apparent signal obtained by MultiGAS.
- In general, we should aim to reduce the subjective choices in the post-processing of MultiGAS data, e.g., the selection of time windows, the means of obtaining background concentrations, the balancing of correlation vs error relative magnitude as the primary quantity to improve. However, the significance of the choices made vary between datasets and we have no quantitative solution as yet. Work in future should acknowledge this subjectivity and attempt to compensate by trying different window lengths, different fitting methods, and examining the impact on the ratios of these choices. Further work is needed between groups to explore how subjective decisions could be reduced or made to follow quantitative principles.

6. Conclusions and Suggested Further Work

The foregoing report has summarised the findings of the Task 5.2 team members, who considered the problem of developing a series of best practice guidelines for the monitoring of volcanic gas emissions in the field, chiefly by UV remote sensing (of SO_2 flux) and in situ MultiGAS measurements (of plume composition). While our efforts have certainly been significantly hampered by our inability to undertake a field campaign together – a consequence of the COVID-19 pandemic, this report does provide a clear series of tractable recommendations that can be shared with the global volcanological community as part of the overall EUROVOLC deliverables package. Our intention is for the above lists of recommendations to provoke debate and inspire further work in this important area. Certainly, there are many issues requiring further work before they are fully understood. Tackling this problem will remain a major focus area for many of us and our colleagues in the wider gas monitoring community.

Briefly, a few areas where we feel particular progress might be made include:

- **Exploration of the combination of traverse, scanning and imaging methods in UV remote sensing**, with this diversity of approaches helping to capture more fully the variability of volcanic emissions as well as the environmental conditions that can hamper their measurement. Such an approach may also lead to reductions in some of the main error sources faced in UV monitoring of SO_2 emissions, such as plume altitude, plume speed, and light dilution.
- **The use of drone-mounted MultiGAS and DOAS instruments to monitor inaccessible volcanic plumes** more readily. Drones offer great advantages in terms of safe access, with beyond visual line of sight (BVLOS) capability particularly exciting in enabling access to hitherto unmeasurable volcanic plumes (e.g. Liu et al., 2020). However, there are associated challenges to overcome, including the rapid transits of plumes made by fixed-wing aircraft (resulting in short acquisition times in the plume) and the turbulence generated by multi-rotor aircraft (influencing mixing of plume with ambient atmosphere).
- **The use of MultiGAS with or without active pumping.** The polytetrafluoroethylene (PTFE) filter used to prevent particles entering the instrument could in fact act as a diffusive barrier, at the entrance of the sampling line, which is kept under a pressure gradient by the pump. This architecture leads to effusion of the plume volume sampled in front of the filter, which is continuously rejuvenated by the local circulation, most often turbulent (Moretti et al., 2020). Some tests and improvements should be carried in the future to better model and recognize all the intervening effects that can mask our search for the original fumarolic composition. In particular, a new MultiGAS architecture must be tested removing filter and possibly the pump.
- **High sampling rate with t90 concerns.** High frequency time series with constant sampling rate (for instance each second) are needed to make the best use of statistical relationships. Moreover, a low-pass filter considering the lowest t90 of the species of the considered ratio should be applied to all measured concentration data in order to overcome the differences in response time between sensors and to capture the gas chemistry pulses well.
- **The multiplication of X/SO_2 ratios and SO_2 flux to calculate per-species emission rates.** Since emission rates of most species of interest in volcanic plumes (H_2O, CO_2, CO, H_2S, HCl) cannot be readily measured by remote sensing methods, fluxes of these species are typically calculated from the combination of composition (ratios) obtained by MultiGAS and independently acquired SO_2 fluxes. This can prove problematic since SO_2 fluxes are often accurate spectroscopic column amounts convolved with wind speeds subject to large errors. These errors then propagate into the other species' emission rates. Two important paths forward might be (1) the improvement of wind speed estimates around active volcanoes (e.g., by drifting drone measurements or particle tracking

algorithms applied to high-speed camera footage of the plume) and (2) the exploration of new methods of calculating fluxes of other species independently (e.g., raster methods with drone-mounted gas sensors, e.g. H_2S fluxes via MultiGAS when SO_2 is absent (as in low-temperature hydrothermal systems for instance, see Allard et al., 2014).

7. References Cited

Aiuppa, A., Moretti, R., Federico, C., Giudice, G., Gurrieri, S., Liuzzo, M., Papale, P., Shinohara, H., Valenza, M., 2007. Forecasting Etna eruptions by real-time observation of volcanic gas composition. Geology. 35 (12), 1115-1118.

Aiuppa, A., Federico, C., Giudice, G., Giuffrida, G., Guida, R., Gurrieri, S., Liuzzo, M., Moretti, R., Papale, P., 2009. The 2007 eruption of Stromboli volcano: insights from real-time measurement of the volcanic gas plume CO2/SO2 ratio. Journal of Volcanology and Geothermal Research, 182 (3-4), 221-230.

Allard, P., Burton, M., Mure, F., 2005. Spectroscopic evidence for a lava fountain driven by previously accumulated magmatic gas. Nature, 433, 407-410.

Allard, P., Aiuppa, A., Beauducel, F., Gaudin, D., Di Napoli, R., Calabrese, S., Parello, F., Crispi, O., Hammouya, G., Tamburello, G., 2014. Steam and gas emission rate from La Soufriere volcano, Guadeloupe (Lesser Antilles): implications for the magmatic supply during degassing unrest. Chemical Geology, 384, 76-93.

Arellano, S.R., Hall, M., Samaniego, P., Le Pennec, J.-L., Ruiz, A., Molina, I., Yepes, H., 2008. Degassing patterns of Tungurahua volcano (Ecuador) during the 1999–2006 eruptive period, inferred from remote spectroscopic measurements of SO2 emissions, Journal of Volcanology and Geothermal Research, 176 (1), 151-162.

Arellano, S., Galle, B., & 38 co-authors, 2021. Synoptic analysis of a decade of daily measurements of SO2 emission in the troposphere from volcanoes of the global ground-based Network for Observation of Volcanic and Atmospheric Change, Earth Syst. Sci. Data, 13, 1167-1188.

Behncke, B., Calvari, S., Giammanco, S., Neri, M., Pinkerton, H., 2008. Pyroclastic density currents resulting from the interaction of basaltic magma with hydrothermally altered rock: an example from the 2006 summit eruptions of Mount Etna, Italy. Bulletin of Volcanology, 70, 1249-1268.

Beirle, S., Lampel., J., Lerot, C., Sihler, H., Wagner, T., 2017. Parameterizing the instrumental spectral response function and its changes by a super=Gaussian and its derivatives. Atmos. Meas. Tech., 10, 581-598.

Bloomfield, P. & Steiger, W., 1983. Least Absolute Derivations, Springer.

Bonforte, A., Bonaccorso, A., Guglielmino, F., Palano, M., Puglisi, G., 2008. Feeding system and magma storage beneath Mt. Etna as revealed by recent inflation/deflation cycles. Journal of Geophysical Research: Solid Earth, 113 (B5).

Burton, M., Oppenheimer, C., Horrocks, L.A., Francis, P.W., 2000. Remote sensing of CO2 and H2O emission rates from Masaya volcano, Nicaragua. Geology, 28 (10), 567-570.

Burton, M., Sawyer, G.M., Granieri, D., 2013. Deep carbon emissions from volcanoes. Reviews in Mineralogy and Geochemistry, 75 (1), 323-354.

Caltabiano, T., R. Romano, and G. Budetta, SO2 measurements at Mount Etna, Sicily, J. Geophys. Res., 99, 12,809-12,811, 1994.

Chance, K., 1998. Analysis of BrO measurements from the global ozone monitoring experiment. Geophys. Res. Lett. 25, 3335–3338

Chiodini, G., Cioni, R., Marini, L., Panichi, C., 1995, Origin of the fumarolic fluids of Vulcano Island, Italy and implications for volcanic surveillance, Bulletin of Volcanology, 57 (2), 99-110.

De Moor, J.M., Aiuppa, A., Avard, G., Wehrmann, H., Dunbar, N., Mueller, C., Tamburello, G., Giudice, G., Liuzzo, M., Moretti, R., Conde, V., Galle, B., 2016. Turmoil at Turrialba volcano (Costa Rica): Degassing and eruptive processes inferred from high-frequency gas monitoring, Journal of Geophysical Research: Solid Earth, 121 (8), 5761-5775.

De Moor, J.M., Kern, C., Avard, G., Mueller, C., Aiuppa, A., Saballos, A., Ibarra, M., LaFemina, P., Protti, M., Fischer, T.P., 2018, A new sulfur and carbon degassing inventory for the Southern Central American Volcanic Arc: the importance of accurate time-series data sets and possible tectonic processes responsible for temporal variations in arc-scale volatile emissions. Geochemistry, Geophysics, Geosystems, 18 (12).

Dodge, Y., 1997. LAD regression for detecting outliers in response and explanatory variables, Journal of Multivariate Analysis, 61, 144-158.

Edmonds, M., Oppenheimer, C., Pyle, D.M., Herd, R.A., Thompson, G., 2003a. SO2 emissions from Soufriere Hills Volcano and their relationship to conduit permeability, hydrothermal interaction and degassing regime. Journal of Volcanology and Geothermal Research, 124 (1-2), 23-43.

Edmonds, M., Herd, R.A., Galle, B., Oppenheimer, C., 2003b. Automated, high time resolution measurements of SO2 flux at Soufrière Hills Volcano, Montserrat. Bull. Volcanol. 65, 578–586.

Edmonds, M., 2008. New geochemical insights into volcanic degassing. Phil. Trans. Roy. Soc. A., 366 (1885).

Edmonds, M., 2021. Geochemical monitoring of volcanoes and the mitigation of volcanic gas hazards, In: Forecasting and Planning for Volcanic Hazards, Risks, and Disasters. Elsevier.

Esse, B., Burton, B., Varnam, M., Kazahaya, R., Salerno, G., 2020. iFit: a simple method for measuring volcanic SO2 without a measured Fraunhofer reference spectrum. Journal of Volcanology and Geothermal Research, 107000.

Fischer, T.P, Giggenbach, W.F., Sano, Y., Williams, S.N., 1998. Fluxes and sources of volatiles discharged from Kudryavy, a subduction zone volcano, Kurile Islands. Earth and Planetary Science Letters, 160 (1-2).

Fischer, T.P. & Aiuppa, A., 2020, Global CO2 emissions from subaerial volcanism---recent progress and future challenges. Geochemistry, Geophysics, Geosystems, 21 (3).

Galle, B., Oppenheimer, C., Geyer, A., McGonigle, A.J.S., Edmonds, M., Horrocks, L., 2003. A miniaturized ultraviolet spectrometer for remote sensing of SO2 fluxes: a new tool for volcano surveillance. Journal of Volcanology and Geothermal Research, 119 (1-4), 241-254.

Galle, B., Johannson, M., Rivera, C., Zhang, Y., Kihlman, M., Kern, C., Lehmann, T., Platt, U., Arellano, S., Hidalgo, S., 2010. Network for Observation of Volcanic and Atmospheric Change (NOVAC)---A global network for volcanic gas monitoring: network layout and instrument description. Journal of Geophysical Research: Atmospheres, 115, D5.

Gaudin, D., Beauducel, F., Coutant, O., Delacourt, C., Richon, P., de Chabalier, J.-B., Hammouya, G., 2016. Mass and heat flux balance of La Soufriere volcano (Guadeloupe) from aerial infrared thermal imaging. Journal of Volcanology and Geothermal Research, 320, 107-116.

Global Volcanism Program, 2007. Report on Stromboli (Italy). (Wunderman, R., eds.). Bulletin of the Global Volcanism Network, 32:4. Smithsonian Institution.

Global Volcanism Program, 2012. Report on Etna (Italy). (Wunderman, R., eds.). Bulletin of the Global Volcanism Network, 37:2. Smithsonian Institution.

Global Volcanism Program, 2021. Report on Stromboli (Italy). (Bennis, K. & Venzke, E., eds.). Bulletin of the Global Volcanism Network, 32:4. Smithsonian Institution.

James, M.R., Carr, B., D'Arcy, F., Diefenbach, A., Dietterich, H., Fornaciai, A., Lev, E., Liu, E., Pieri, D., Rodgers, M., Smets, B., Terada, A., von Aulock, F., Walter, T., Wood, K., Zorn, E., 2020. Volcanological applications of unoccupied aircraft systems (UAS): developments, strategies and future challenges. Volcanica, 3 (1), 67-114.

Jessop, D.E., Moune, S., Moretti, R., Gibert, D., Komorowski, J.-C., Robert, V., Heap, M.J., Bosson, A., Bonifacie, M., Deroussi, S., Dessert, C., Rosas-Carbajal, M., Lemarchand, A., Burtin, A., 2021. A multi-decadal view of the heat and mass budget of a volcano in unrest: La Soufriere de Guadeloupe (French West Indies). Bulletin of Volcanology, 83 (3).

Hoff, R.M., and M.M. Millan, Remote SO2 Mass Flux Measurements Using COSPEC, J. Air Pollution Control Association, 31, 381-384

Kazahaya, R., Mori, T., Kazahaya, K., Hirabayashi, J-.i., 2008. Computed tomography reconstruction of SO2 concentration distribution in the volcanic plume of Miyakejima, Japan, by airborne traverse technique using three UV spectrometers. Geophysical Research Letters, 35 (13).

Kern, C., Deutschmann, T., Vogel, L., Wohrbach, M., Wagner, T., Platt, U., 2010. Radiative transfer corrections for accurate spectroscopic measurements of volcanic gas emissions. Bulletin of Volcanology, 72 (2), 233-247

Kern, C., Deutschmann, T., Werner, C., Sutton, A.J., Elias, T., Kelly, P.J., 2012. Improving the accuracy of SO2 column densities and emission rates obtained from upward-looking UV-spectroscopic measurements of volcanic plumes by taking realistic radiative transfer into account. Journal of Geophysical Research: Atmospheres, 117, D20.

Kern, C., Werner, C., Elias, T., Sutton, A.J., Lubcke, P., 2013. Applying UV cameras for SO2 detection to distant or optically thick volcanic plumes. Journal of Volcanology and Geothermal Research, 262, 80-90.

Liu, E.J., A. Aiuppa, A. Alan, S. Arellano, M. Bitetto, N. Bobrowski, S. Carn, R. Clarke, E. Corrales, J.M. de Moor, J.A. Diaz, M. Edmonds, T.P. Fischer, J. Freer, G.M. Fricke, B. Galle, G. Gerdes, G. Giudice, A. Gutmann, C.S.L Hayer, I. Itikarai, J. Jones, E. Mason, B.T. McCormick Kilbride, K. Mulina, S. Nowicki, K. Rahilly, T. Richardson, J. Rüdiger, C.I. Schipper, I.M. Watson, K. Wood, Aerial strategies advance volcanic gas measurements at inaccessible, strongly degassing volcanoes, Science Advances, 6 (44).

Malicet, J., D. Daumont, J. Charbonnier, C. Parisse, A. Chakir, and J. Brion (1995), Ozone UV spectroscopy: II. Absorption cross-sections and temperature dependence, J. Atmos. Chem., 21(3), 263–273, doi:10.1007/BF00696757.

Malinconico, L.L., On the variation of SO2 emission from volcanoes, J. Volcanol. Geotherm. Res., 33, 231-237, 1987.

Mason, E., Edmonds, M., Turchyn, A.V., 2017. Remobilization of crustal carbon may dominate volcanic arc emissions, Science, 357 (6348).

Mather, T. A., D. M. Pyle, V. I. Tsanev, A. J. S. McGonigle, C. Oppenheimer, and A. G. Allen (2006), A reassessment of current volcanic emissions from the Central American arc with specific examples from Nicaragua, J. Volcanol. Geotherm. Res., 149(3–4), 297–311, doi:10.1016/j.jvolgeores.2005.07.021

McGonigle, A.J.S., Oppenheimer, C., Hayes, A.R., Galle, B., Edmonds, M., Caltabiano, T., Salerno, G., Burton, M., 2003. Volcanic sulphur dioxide fluxes from Etna, Vulcano and Stromboli measured with an automated scanning ultraviolet spectrometer. J. Geophys. Res. 108, B9.

McGonigle, A. J. S., Inguaggiato, S., Aiuppa, A., Hayes, A. R., & Oppenheimer, C. (2005a). Accurate measurement of volcanic SO2 flux: Determination of plume transport speed and integrated SO2 concentration with a single device. Geochem., Geophys., Geosyst., 6 (2).

McGonigle, A.J.S., Pering, T.D., Wilkes, T.C., D'Aleo, R., Bitetto, M., Aiuppa, A., Wilmott, J.R., 2017. Ultraviolet imaging of volcanic plumes: a new paradigm in volcanology. Geosciences, 7 (3), 68.

Moretti, R., Moune, S., Robert, V., Jessop, D.E., Didier, T., Bonifacie, M., Komorowski, J.-C., 2020, Intercomparison of geochemical techniques at La Soufrière de Guadeloupe (FWI) volcano: their advantages and their limits over a long-standing unrest, Italian Journal of Geosciences, accepted

Mori, T., Mori, T., Kazahaya, K., Ohwada, M., Hirabayashi, J., & Yoshikawa, S. (2006). Effect of UV scattering on SO2 emission rate measurements. Geophys. Res. Lett., 33 (17).

Mori, T., & Burton, M. (2006). The SO2 camera: A simple, fast and cheap method for ground-based imaging of SO2 in volcanic plumes. Geophys. Res. Lett., 33 (24).

Moune, S., R. Moretti, A. Burtin, D. E. Jessop, T. Didier, V. Robert, M. Bonifacie, G. Tamburello, J.C. Komorowski, P. Allard, M. Buscetti; submitted to Frontiers, Gas monitoring of volcanic-hydrothermal plumes in a tropical environment: the case of La Soufrière de Guadeloupe unrest volcano (FWI)

Moussallam, Y., Peters, N., Masias, P., Apaza, F., Barnie, T., Schipper, C.I., Curtis, A., Tamburello, G., Aiuppa, A., Bani, P., Giudice, G., Pieri, D., Gerard Davies, A., Oppenheimer, C., 2017. Magmatic gas percolation through the old lava dome of El Misti volcano. Bulletin of Volcanology, 79 (6), 46.

Neri, M., and V. Acocella (2006), The 2004–05 Etna eruption: Implications for flank deformation and structural behaviour of the volcano, *J. Volcanol. Geotherm. Res.*, **158**, 195– 206.

Oppenheimer, C., Scaillet, B., Martin, R.S., 2011. Sulfur degassing from volcanoes: source conditions, surveillance, plume chemistry and earth system impacts. Reviews in Mineralogy and Geochemistry, 73 (1), 363-421.

Peters, N., Hoffmann, A., Barnie, T., Herzog, M., Oppenheimer, C., 2015. Use of motion estimation algorithms for improved flux measurements using SO2 cameras. Journal of Volcanology and Geothermal Research, 300, 58-69.

Platt, U., & Stutz, J. (2008). Differential Optical Absorption Spectroscopy. Springer-Verlag.

Platt, U., Bobrowski, N., & Butz, A. (2018). Ground-based remote sensing and imaging of volcanic gases and quantitative determination of multispecies emission fluxes. Geosciences, 8 (2), 44.

Roberts, T.J., Saffell, J.R., Oppenheimer, C., Lurton, T., 2014. Electrochemical sensors applied to pollution monitoring: measurement error and gas ratio bias---a volcano plume case study. Journal of Volcanology and Geothermal Research, 281, 85-96.

Rufus, J., Stark, G., Smith, P. L., Pickering, J. C., & Thorne, A. P. (2003). High-resolution photoabsorption cross section measurements of SO2, 2: 220 to 325 nm at 295 K. J. Geophys. Res.: Planets, 108 (E2), 15.

Salerno, G. G., Burton, M. R., Oppenheimer, C., Caltabiano, T., Randazzo, D., Bruno, N., et al. (2009a). Three-years of SO2 flux measurements of Mt. Etna using an automated UV scanner array: comparison with conventional traverses and uncertainties in flux retrieval. J. Volcanol. Geotherm. Res. 183, 76–83.

Shinohara, H., 2005. A new technique to estimate volcanic gas composition: plume measurements with a portable multi-sensor system. Journal of Volcanology and Geothermal Research, 143 (4), 319-333.

Shinohara, H., 2013. Volatile flux from subduction zone volcanoes: insights from a detailed evaluation of the fluxes from volcanoes in Japan. Journal of Volcanology and Geothermal Research, 268, 46-63.

Sparks, R.S.J., Biggs, J., Neuberg, J.W., 2012. Monitoring volcanoes. Science, 335 (6074), 1310-1311.

Stoiber, R.E., Malinconico, L.L., Williams, S.N., 1983. Use of the correlation spectrometer at volcanoes. In: Tazieff, H., Sabroux, J.C. (Eds.), Forecasting Volcanic Events. Elsevier, Amsterdam, pp. 425–444.

Stoiber, R.E., Williams, S.N., Huebert, B., 1987. Annual contribution of sulfur dioxide to the atmosphere by volcanoes. Journal of Volcanology and Geothermal Research, 33 (1-3), 1-8.

Symonds, R.B., Gerlach, T.M., Reed, M.H., 1994. Magmatic gas scrubbing: implications for volcano monitoring, Journal of Volcanology and Geothermal Research, 108 (1-4), 303-341.

Tamburello, G., Kantzas, E.P., McGonigle, A.J.S., Aiuppa, A., Giudice, G., 2011. UV camera measurements of fumarole field degassing (La Fossa crater, Vulcano Island). Journal of Volcanology and Geothermal Research, 199 (1-2), 47-52.

Tamburello, G., 2015. Ratiocalc: software for processing data from multicomponent volcanic gas analyzers. Computers & Geosciences, 82, 63-67.

Tamburello, G., Moune, S., Allard, P., Venugopal, S., Robert, V., Rosas-Carbajal, M., Deroussi, S., Kitou, G.-T., Didier, T., Komorowski, J.-C., Beauducel, F., De Chabalier, J.-B., Le Marchand, A., Le Friant, A., Bonifacie, M., Dessert, C., Moretti, R., 2019. Spatio-temporal relationships between fumarolic activity, hydrothermal fluid circulation and geophysical signals at an arc volcano in degassing unrest: La Soufriere of Guadeloupe (French West Indies), Geosciences, 9 (11), 480.

Vandaele, A. C., P. C. Simon, J. M. Guilmot, M. Carleer, and R. Colin (1994), SO2 absorption cross section, measurement in the UV using a Fourier transform spectrometer, J. Geophys. Res., 99(D12), 25,599–25,605, doi:10.1029/94JD02187.

Varnam, M., Burton, M., Esse, B., Kazahaya, R., Salerno, G., Caltabiano, T., & Ibarra, M. (2020). Quantifying Light Dilution in Ultraviolet Spectroscopic Measurements of Volcanic SO2 Using Dual-Band Modelling. Front. Earth Sci, 8, 468 doi:10.3389/feart.2020.528753

Vaselli, O., Tassi, F., Duarte, E., Fernandez, E., Poreda, R.J., Delgado Huertas, A., 2010. Evolution of fluid geochemistry at the Turrialba volcano (Costa Rica) from 1998 to 2008. Bulletin of Volcanology, 72 (4), 397-410.

Voigt, S., J. Orphal, K. Bogumil, and J.P. Burrows, "The temperature dependence (203-293 K) of the absorption cross sections of O3 in the 230-850 nm region measured by Fourier-transform spectroscopy", J. Photochem. Photobiol. A: Chem. 143, 1-9 (2001); DOI: 10.1016/S1010-6030(01)00480-4

Werner, C., Kelly, P.J., Doukas, M., Lopez, T., Pfeffer, M., McGimsey, R., Neal., C., 2013. Degassing of CO2, SO2 and H2S associated with the 2009 eruption of Redoubt volcano, Alaska. Journal of Volcanology and Geothermal Research, 259, 270-284.

Werner, C., Fischer, T.P., Aiuppa, A., Edmonds, M., Cardellini, C., Carn., S.A., Chiodini, G., Cottrell, E., Burton, M., Shinohara, H., Allard, P., 2019. Carbon dioxide emissions from subaerial volcanic regions. In: Deep Carbon: Past to Present (eds Orcutt, B.N. et al.), Cambridge University Press.

Wright, T., Burton, M., Pyle, D., & Caltabiano, T. (2008). Scanning tomography of SO2 distribution in a volcanic gas plume. Geophys. Res. Lett., 35 (17) doi:10.1029/2008GL034640

Williams-Jones, G., Stix, J., Hickson, C., 2008. The COSPEC Cookbook: making SO2 measurements at active volcanoes. IAVCEI, Methods in Volcanology, vol. 1.